



UNIVERSITY of
DENVER

NATURAL SCIENCES & MATHEMATICS

Department of Chemistry and Biochemistry

November 4, 2016

Dear Associate Editor Dr. Surratt,

Re: Revisions of acp-2016-743 by Gosselin et al.

Here you will find a summary of revisions for our recently reviewed manuscript. All three referees recommended publication after relatively minor changes and comments. We have responded point-by-point to these comments and are confident that the manuscript is improved and ready for acceptance.

Attached within this document you will find documents in the following order:

- Point-by-point responses to Referees #2, 3, 4 (copied directly from documents uploaded to ACP)
- Revised manuscript (with changes highlighted in yellow for all changes requested by referees and in green for all other changes)
- Manuscript supplement

With these changes we hope you will find the revised manuscript soon acceptable for publication.

Best Regards,

A handwritten signature in black ink that reads "J. Alex Huffman".

J. Alex Huffman, Ph.D.
Assistant Professor
Alex.Huffman@DU.edu

1 **Response to referee comment on acp-2016-743 by Gosselin et al.**

2
3 **Anonymous Referee #2**

4 Received and published: 13 October 2016

5
6 Note regarding document formatting: black text shows original referee comment, blue text shows
7 author response, and red text shows quoted manuscript text. Changes to manuscript text are
8 shown as *italicized and underlined*. All line numbers refer to discussion/review manuscript.
9

10 **General Comments:** The manuscript entitled “Fluorescent Bioaerosol Particle, Molecular Tracer, and
11 Fungal Spore Concentrations during Dry and Rainy Periods in a SemiArid Forest” by Gosselin et al.
12 reports correlations of fluorescent aerosol particles of UV-APS and WIBS-3 with molecular tracers of
13 fungal spores and bacteria. This study provides further investigations of the detection ability of UV-LIF
14 instruments of fungal spores. In general, the manuscript was well written and the analysis of the data was
15 well performed. I recommend this manuscript to be accepted for publication after minor revisions.
16

17 **Author response:** We thank the referee for his/her positive assessment and summary.
18

19 **Specific Comments:**

20 Comment 1: In the last paragraph of Introduction and the Discussion sections, the authors declared that
21 this is the first comparison of online UV-LIF with organic molecular tracers measurements. In fact, a
22 recent study has also made such comparisons between WIBS and fungal spore tracers (see Yue et al.,
23 2016, Sci. Rep.).
24

25 We thank the referee for pointing out this reference that we have now included at L127.
26 The Yue et al. paper indeed briefly presents arabitol and mannitol concentrations and also
27 shows WIBS data during one rain event, but does so by showing only qualitative
28 relationships between WIBS and tracer measurements without presenting any
29 quantitative correlations. We have edited the text at L132 to the following to be more
30 accurate with respect to the inclusion of the Yue et al. reference:

31 “This study *of ambient aerosol* represents the *first quantitative comparison of real-time aerosol*
32 *UV-LIF instruments with molecular tracers or culturing.*”
33

34 The Yue paper is also discussed and references in the text at L480:

35 “*More recently, Yue et al. (2016) studied a rain event in Beijing and observed increased*
36 *polyol concentrations at the onset of the rain. The observed mannitol concentration (45*
37 *ng m⁻³) was approximately consistent with observations reported here and with previous*
38 *reports, while the arabitol concentration values observed were approximately an order*
39 *of magnitude lower (0.3 ng m⁻³).*”
40

41
42 Comment 2: In part 2.2 Online fluorescent instruments (Line 174 – 176), the fluorescent detection bands
43 for WIBS-3 should be λ_{em} 310 – 400 nm and λ_{em} 400 – 600 nm (see Gabey et al., 2010, ACP). Please
44 clarify it.
45

46 The WIBS-3 was not a commercialized instrument and so different models had slightly different
47 detector properties. Crawford et al. (2014) reports the following parameter for the PMT detectors:
48 “excitation wavelengths centred at 280 ± 10 nm and 370 ± 20 nm” and emission in “one of two
49 bands that do not overlap the excitation emission, 320–400 nm and 410–650 nm.” We have

50 adjusted the lower bound of the FL1 emission channel from 310 nm to 320 nm to match the
51 Crawford et al. values (L175-176).

52
53 Comment 3: Line 205: Provide references for “One important difference between the models is that the
54 WIBS-3 exhibits comparatively weak FL1 and FL2 signals with respect to the more updated models, and
55 is thus more influenced by FL3”.

56
57 We have clarified the text after L205:

58 ~~“One important difference between the models is that the WIBS-3 exhibits comparatively weak~~
59 ~~FL1 and FL2 signals with respect to the more updated models, and is thus more influenced by~~
60 ~~FL3. This results in a different break-down of *optical chamber design and filters of the WIBS-4*~~
61 ~~*models were updated to enhance the overall sensitivity of the instrument (Crawford et al., 2014).*~~
62 ~~*Additionally, slight differences in detector gain between models and individual units can impact*~~
63 ~~*the relative sensitivity of the fluorescence channels. . This may result in differences in fluorescent*~~
64 ~~*channel intensity between instrument models, as will be discussed later.”*~~

65
66 Comment 4: In Figure 5 (e, f), the unit for WIBS C11 FAP was given as mass concentration. How do the
67 authors convert the number concentrations to mass concentrations for WIBS-3? Such information should
68 be provided in the Methods section.

69
70 For all mass concentration data reported in the manuscript we took UV-APS or WIBS-3 number
71 size distributions, assuming spherical particles with unit density, and converted to mass
72 distributions (mass = number x $\frac{4}{3} \pi \times r^2$), where r is the particle diameter. Integrated mass
73 concentrations were calculated by integrating the total mass between 0.5 and 15 μm . This process
74 is detailed in the discussion version of the paper at L159-167, but has been revised slightly as
75 detailed below:

76 ~~“Total particle number size distributions (irrespective of fluorescence properties) obtained from~~
77 ~~the UV-APS *and WIBS* were converted to mass distributions ~~using *assuming spherical particles*~~~~
78 ~~*of unit particle mass density as a first approximation for all direct comparisons with tracer mass*~~
79 ~~*and, unless otherwise stated.”*~~

80 81 **References**

82
83 Crawford, I., Robinson, N. H., Flynn, M. J., Foot, V. E., Gallagher, M. W., Huffman, J. A., Stanley, W.
84 R., and Kaye, P. H.: Characterisation of bioaerosol emissions from a Colorado pine forest: results from
85 the BEACHON-RoMBAS experiment, Atmos Chem Phys, 14, 8559-8578, 10.5194/acp-14-8559-2014,
86 2014.

1 **Response to referee comment on acp-2016-743 by Gosselin et al.**

2
3 **Anonymous Referee #3**

4 Received and published: 5 October 2016

5
6 Note regarding document formatting: black text shows original referee comment, blue text shows
7 author response, and red text shows quoted manuscript text. Changes to manuscript text are
8 shown as *italicized and underlined*. All line numbers refer to discussion/review manuscript.
9

10 **General Comments:** The manuscript is very well written and I believe of great relevance to the bioaerosol
11 scientific community. The authors present very interesting and novel work comparing data from modern
12 Light/Laser induced fluorescence (LIF) instruments with molecular tracers such as arabitol and mannitol.
13 The paper also attempts to display the data in new ways scaling particle number to mass concentrations.
14 The paper is very well cited and builds well on previous work. Thus I believe the paper should be
15 published upon the correction of some minor technical/specific issues discussed below.
16

17 **Author response:** We thank the referee for his/her positive assessment and summary.
18

19 **Specific Comments:**

20 Comment 1: L62-63 “For example, asthma and allergies have shown notable increases during
21 thunderstorms due to elevated bioaerosol concentrations” This is indeed true however allergic rates have
22 been climbing in recent years and I feel this should be incorporated. I suggest using the reference.
23 Linneberg, A., 2011. The increase in allergy and extended challenges. Allergy, 66(s95), pp.1-3.
24

25 The Linneberg reference was added to L62.
26

27 Comment 2: L139 should H₂O have a sub-scripted 2
28

29 This was corrected in the revised manuscript.
30

31 Comment 3: Were the differences in sampling lines of the WIBS and UV-APS calculated? Reynolds
32 number for instance?
33

34 We did not calculate the Reynolds number or quantify possible difference in the two sampling
35 lines. The lines from the inlets were somewhat different in length (~4.5 m for the UV-APS and
36 <1 m for the WIBS), but both were arranged to minimize bends and were oriented vertically.
37 Thus, the differences in particle number concentration from the inlets and lines is likely minimal.
38

39 Comment 4: Were all particles assumed to be spherical for the density calculations or was the WIBS
40 ability to determine shape utilized?
41

42 All particles were assumed to be spherical for particle mass calculations. Particle morphology
43 could impact particle mass calculations, however, the asymmetry factor (AF) provided by the
44 WIBS has not been characterized sufficiently to understand the relationship of this parameter to
45 particle morphology. As a result, we did not utilize AF. To clarify ambiguity, the text was revised
46 at L160-162 as follows:

47 “Total particle number size distributions (irrespective of fluorescence properties) obtained from
48 the UV-APS *and WIBS* were converted to mass distributions ~~using assuming spherical particles~~
49 *of unit particle mass density as a first approximation for all direct comparisons with tracer mass*
50 *and, unless otherwise stated.*”
51

52 Comment 5: Do you believe that cluster 1 is solely a fungal spore cluster, given its size range overlaps
53 with that of some bacteria?
54

55 The organization of clusters from the raw data is a function of the mathematical algorithms
56 utilized and is relatively robust. The assignment of names or sources to the derived clusters is
57 much more uncertain. While Crawford et al. (2015) assigned Cluster 1 to be fungal spores, this
58 should be taken loosely. It is very possible that some fraction of non-fungal particles have been
59 conflated with this cluster. Without direct comparative evidence there is no way to confidently
60 know the source or category of each particle. For example, even the cluster assignment of even
61 polystyrene latex particles of known type was reported as only 98% in a previous publication
62 (Crawford et al., 2015). To clarify this point we have added the following text to the end of L203.
63 *“It should be noted that assignment of names and approximate origin (e.g. fungal spores or*
64 *bacteria) to clusters is approximate and does not imply particle homogeneity. Each cluster likely*
65 *contains a small percentage of contaminating particles. For more details see Robinson et al.*
66 *(2013) and Crawford et al. (2015).”*
67

68 Comment 6: Why was a rainfall accumulation threshold of greater than 0.201 chosen?
69

70 A threshold of 0.201 represents a normalized and unitless value that takes into account both
71 disdrometer and tipping bucket measurements. This value was chosen arbitrarily based on the
72 following reasoning. Rain events that presented <0.201 often did not coincide with other
73 indicators of rain such as increased fluorescent particle concentration and RH. When the
74 threshold value was increased to 0.201 we observed more continuity in the measurements that are
75 indicative of rain events.
76

77 Comment 7: What did the correlations look like before the manual reclassification of some of the rain/dry
78 periods? How much did this effect it?
79

80 Regarding the correlations, manual reclassification by wetness category increased the R^2 values
81 in all cases. For example, prior to reclassification the mass correlation of arabitol with WIBS
82 cluster 1 during rainy periods was 0.77 after reclassification the R^2 value was 0.82. This trend of
83 increased R^2 was observed with other correlations for both rainy and dry periods.
84

85 Comment 8: L 430-431. The Hill 2009 reference does talk about increased wetness effecting the
86 fluorescent properties in comparison to dry samples however in this study wet samples were particles
87 suspended in solution rather than particles at higher relative humidity's. **(a)** I believe that this line should
88 be rewritten. **(b)** Do you believe the particles sampled during wet periods to be in droplets or to have
89 increased moisture content? **(c)** Could a moistened PBAP have increased fluorescence due to fluorescent
90 compounds being extracted/leached to its surface?
91

92 These are interesting questions that were somewhat beyond the scope of the ambient study
93 performed here and thus we did not fully investigate them.

94 **(a)** Taking this comment into account we revised this sentence (L 430-431) to be more accurate:
95 *“This could impact the fluorescence properties of the fungal spore particles that have different*
96 *amounts of adsorbed or associated water (Hill et al., 2009; 2013; 2015).”*

97 **(b)** As far as the moisture content of individual spores, we have no direct evidence either way. It
98 is possible that some of the spores were fully contained within water droplets, either as a by-
99 product of the high RH and deliquescence or because spores were actively ejected by fungus and
100 thus encased in a small droplet. Upon interrogation within the UV-LIF instruments, however, the
101 spores were almost surely not activated within a droplet, because of the size ranges observed. If
102 they were encased within a droplet the average size would have likely been too large for the UV-

103 LIF instruments to sample efficiently and we would not have observed the dominant 2-6 μm
104 modes.

105 (c) We are aware of no studies that directly link increased fluorescence with the leaching of
106 fluorescent compounds from the interior to the surface of a particle. However, (Hill et al., 2013;
107 2015) showed that the water content associated with bacterial aerosols significantly affected their
108 fluorescence properties, which led to the brief statement quoted above.

109
110 Comment 9: Was there much difference in fluorescent intensity for FAP on Dry and Wet periods?

111 We did not perform this analysis as a part of this study. But, intrigued by the referee's question
112 we calculated average fluorescence intensity from two samples (one Rainy, one Dry) as
113 examples. Hi Vol sample 8 was a dry sample with intensities as follows: FL 1, 872 ± 718 ; FL 2,
114 654 ± 277 ; FL 3, 497 ± 347 . Hi Vol sample 16 was a rainy sample with intensities as follows: FL
115 1, 1687 ± 613 ; FL 2, 740 ± 333 ; FL 3, 707 ± 493 . In this example, FL1 intensity increased by a
116 factor of 2, FL2 intensity only nominally increased, and FL3 intensity increased by ~40%.

117
118 Comment 10:

- 119 • L555 Should "Figures 6 c-f" read "Figures 6 d-f"?
120 ○ Corrected
- 121 • L560 Should "Figure 6 c, d" read "Figure 6 d, e"?
122 ○ Corrected
- 123 • L567 Should "Figure 6 e, f" read "Figure 6 g, h"?
124 ○ Corrected

125
126 Comment 11: For the total particulate matter mass concentrations why did you not use the high volume
127 sampler samples to determine the total mass? Instead of the UV-APS measurements.

- 128
129 • Filter mass was not measured before and after sampling and so it was not possible to estimate
130 total particle mass using these filters. As a result, we estimated particle mass using the integrated
131 mass from a particle sizing instrument.

132
133 Comment 12: You mention *Cladosporium* are generally present/released at dry periods was there any
134 evidence that this occurred during this campaign?

135
136 The observation that *Cladosporium* spores are present in highest concentration during dry periods
137 has been reported many times and is generally well accepted (De Groot, 1968; Oliveira et al.,
138 2009). For example, it was shown for a study in rural Ireland that both WIBS and UV-APS
139 instruments poorly detected *Cladosporium* particles (Healy et al., 2014). Unfortunately we have
140 no direct observations of this from the campaign. We collected particle by impaction (Sporewatch
141 drum sampler), but it malfunctioned and we have no direct microscopy samples to show relative
142 spore concentrations. The DNA analysis shows relative diversity, but does not provide
143 quantitative evidence that can support the suggestion that *Cladosporium* was present primarily
144 during dry periods.

145 146 **References**

- 147
148 Crawford, I., Ruske, S., Topping, D., and Gallagher, M.: Evaluation of hierarchical agglomerative cluster
149 analysis methods for discrimination of primary biological aerosol, *Atmos Meas Tech*, 8, 4979-4991,
150 2015.
- 151 De Groot, R.: Diurnal cycles of air-borne spores produced by forest fungi, *Phytopathology*, 58, 1223-
152 1229, 1968.

153 Healy, D., Huffman, J., O'Connor, D., Pöhlker, C., Pöschl, U., and Sodeau, J.: Ambient measurements of
154 biological aerosol particles near Killarney, Ireland: a comparison between real-time fluorescence and
155 microscopy techniques, *Atmos Chem Phys*, 14, 8055-8069, 2014.

156 Hill, S. C., Mayo, M. W., and Chang, R. K.: Fluorescence of bacteria, pollens, and naturally occurring
157 airborne particles: excitation/emission spectra, DTIC Document, 2009.

158 Hill, S. C., Pan, Y.-L., Williamson, C., Santarpia, J. L., and Hill, H. H.: Fluorescence of bioaerosols:
159 mathematical model including primary fluorescing and absorbing molecules in bacteria, *Optics Express*,
160 21, 22285-22313, 10.1364/oe.21.022285, 2013.

161 Hill, S. C., Williamson, C. C., Doughty, D. C., Pan, Y.-L., Santarpia, J. L., and Hill, H. H.: Size-
162 dependent fluorescence of bioaerosols: Mathematical model using fluorescing and absorbing molecules in
163 bacteria, *Journal of Quantitative Spectroscopy and Radiative Transfer*, 157, 54-70,
164 <http://dx.doi.org/10.1016/j.jqsrt.2015.01.011>, 2015.

165 Oliveira, M., Ribeiro, H., Delgado, J., and Abreu, I.: The effects of meteorological factors on airborne
166 fungal spore concentration in two areas differing in urbanisation level, *International journal of*
167 *biometeorology*, 53, 61-73, 2009.

168
169

1 **Response to referee comment on acp-2016-743 by Gosselin et al.**

2
3 **Anonymous Referee #4**

4 Received and published: 6 October 2016

5
6 Note regarding document formatting: black text shows original referee comment, blue text shows
7 author response, and red text shows quoted manuscript text. Changes to manuscript text are
8 shown as *italicized and underlined*. All line numbers refer to discussion/review manuscript.
9

10 **General Comments:** The article is of high quality providing a novel information relevant to the ACP
11 addressing the atmospheric biological (fungal) tracers. The novelty is in correlations reported for periods
12 affected by rain between fungal biomarkers obtained from offline measurements and fluorescent aerosol
13 particle concentrations obtained by direct online measurements. The description of experimental work is
14 sound and detailed supporting the good quality of the paper.
15

16 Author response: We thank the referee for his/her positive assessment and summary.
17

18 **Specific Comments:**

19 (Note that referee comments have been labeled by number and chopped by individual referee-
20 thought so they can be dealt with in a clear sequence)
21

22 Comment 1: In my opinion, the article would gain if additional data with regard to total PM mass
23 concentrations were reported. For example Table 3 presents % contribution of biomarkers with regard to
24 particulate matter and spore mass. The estimated PM mass data presented along with the rest of the data
25 would help to clarify relationship to overall chemical characterization of PM if The data reported are
26 comprehensive.
27

28 Total particle mass ($\mu\text{g m}^{-3}$) was added to Table S4.
29

30 Comment 2: Still are there also data available for the same period reporting on the occurrence of organic
31 carbon and thus allowing for discussion of traditionally reported chemical characterization of organic
32 particulate matter?
33

34 Total organic carbon measurements for the same sampling periods are not available. We asked
35 several BEACHON-RoMBAS collaborators, but did not find such data available.
36

37 Comment 3: Authors report on taxonomic differences in fungal DNA during wet and dry periods. Could
38 such differences be attributed to the ability of different fungal species to survive in different humidity
39 conditions?
40

41 It is certainly plausible that certain fungal species are more likely to survive in wet conditions, or
42 vice versa, and that the rate of emission of a given species will be lower during conditions
43 unfavorable for survivability. However, unless the DNA were to become damaged, which is
44 unlikely, the molecular genomic analyses will still detect the presence of the species. So this
45 process could be involved on a small level, but it is unlikely that survivability would directly
46 impact the observations.
47

1
2 **Title:** Fluorescent Bioaerosol Particle, Molecular Tracer, and Fungal Spore Concentrations during Dry
3 and Rainy Periods in a Semi-Arid Forest
4

5
6 **Authors:** Marie Ila GOSSELIN^{1,2}, Chaturika M Rathnayake³, Ian Crawford⁴, Christopher Pöhlker²,
7 Janine Fröhlich-Nowoisky², Beatrice Schmer², Viviane R. Després⁵, Guenter Engling⁶, Martin
8 Gallagher⁴, Elizabeth Stone³, Ulrich Pöschl², and J. Alex Huffman^{1*}
9

10 ¹Department of Chemistry and Biochemistry, University of Denver, Denver, Colorado, USA

11 ²Max Planck Institute for Chemistry, Multiphase Chemistry and Biogeochemistry Departments, Mainz,
12 Germany

13 ³Department of Chemistry, University of Iowa, Iowa City, IA 52246, USA

14 ⁴Centre for Atmospheric Science, SEAES, University of Manchester, Manchester, UK

15 ⁵Institute of General Botany, Johannes Gutenberg University, Mainz, Germany

16 ⁶Division of Atmospheric Sciences, Desert Research Institute, Reno, NV, USA
17

18 * Correspondence to: alex.huffman@DU.edu
19

20 **Abstract:**

21 Bioaerosols pose risks to human health and agriculture and may influence the evolution of mixed-phase
22 clouds and the hydrological cycle on local and regional scales. The availability and reliability of methods
23 and data on the abundance and properties of atmospheric bioaerosols, however, are rather limited. Here
24 we analyze and compare data from different real-time Ultraviolet Laser/Light Induced Fluorescence (UV-
25 LIF) instruments with results from a culture-based spore sampler and offline molecular tracers for
26 airborne fungal spores in a semi-arid forest in the Southern Rocky Mountains of Colorado. Commercial
27 UV-APS (Ultraviolet Aerodynamic Particle Sizer) and WIBS-3 (Wideband Integrated Bioaerosol Sensor,
28 Version 3) instruments with different excitation and emission wavelengths were utilized to measure
29 fluorescent aerosol particles (FAP) during both dry weather conditions and periods heavily influenced by
30 rain. Seven molecular tracers of bioaerosols were quantified by analysis of total suspended particle (TSP)
31 high-volume filter samples using High Performance Anion Exchange Chromatography with Pulsed
32 Amperometric Detection (HPAEC-PAD). From the same measurement campaign Huffman et al. (2013)
33 previously reported dramatic increases in total and fluorescence particle concentrations during and
34 immediately after rainfall and also showed a strong relationship between the concentrations of FAP and
35 ice nuclei (Huffman et al., 2013; Prenni et al., 2013). Here we investigate molecular tracers and show that
36 during rainy periods the atmospheric concentrations of arabitol ($35.2 \pm 10.5 \text{ ng m}^{-3}$) and mannitol ($44.9 \pm$
37 13.8 ng m^{-3}) were 3-4 times higher than during dry periods. During and after rain the correlations between
38 FAP and tracer mass concentrations were also significantly improved. Fungal spore number
39 concentrations on the order of 10^4 m^{-3} , accounting for 2-4% of TSP mass during dry periods and 17-23%
40 during rainy periods, were obtained from scaling the tracer measurements and from multiple analysis
41 methods applied to the UV-LIF data. Endotoxin concentrations were also enhanced during rainy periods,
42 but showed no correlation with FAP concentrations. Average mass concentrations of erythritol,
43 levoglucosan, glucose, and (1→3)-β-D-glucan in TSP samples are reported separately for dry and rainy
44 weather conditions. Overall, the results indicate that UV-LIF measurements can be used to infer fungal
45 spore concentrations, but substantial development of instrumental and data analysis methods seems
46 required for improved quantification.

1. Introduction

Primary biological aerosols particles (PBAP) are of keen interest within the scientific community, partially because methods for their quantification and characterization are advancing rapidly (Huffman and Santarpia, 2016; Sodeau and O'Connor, 2016). The term PBAP, or equivalently bioaerosol, generally comprises several classes of airborne biological particles including viruses, bacteria, fungal spores, pollen and their fragments (Després et al., 2012; Fröhlich-Nowoisky et al., 2016). Fungal spores are of particular atmospheric interest because they can cause a variety of deleterious health effects in humans, animals, and agriculture, and it has been shown that they can represent a significant fraction of total organic aerosol emissions (Deguillaume et al., 2008; Gilardoni et al., 2011; Madelin, 1994), especially in tropical regions (Elbert et al., 2007; Huffman et al., 2012; Pöschl et al., 2010; Zhang et al., 2010). Current estimates of the atmospheric concentration of fungal spores range from 10^0 to more than 10^4 m^{-3} (Frankland and Gregory, 1973; Gregory and Sreeramulu, 1958; Heald and Spracklen, 2009; Hummel et al., 2015; Sesartic and Dallafior, 2011). Fungal spores may also impact the hydrological cycle as giant cloud condensation nuclei (GCCN) or as ice nuclei (IN) (Haga et al., 2013; Morris et al., 2013; Sesartic et al., 2013). Additionally, several classes of bioaerosols and their constituent components, such as (1→3)- β -D-glucan and endotoxins, have been implicated in respiratory distress and allergies (Burger, 1990; Douwes et al., 2003; Laumbach and Kipen, 2005; Linneberg, 2011; Pöschl and Shiraiwa, 2015). For example, asthma and allergies have shown notable increases during thunderstorms due to elevated bioaerosol concentrations (Taylor and Jonsson, 2004) especially when attributed to fungal spores (Allitt, 2000; Dales et al., 2003).

Molecular tracers have long been utilized as a means of aerosol source tracking (Schauer et al., 1996; Simoneit and Mazurek, 1989; Simoneit et al., 2004). In recent years, analysis of molecular tracers has been utilized for the quantification of PBAP in atmospheric samples and has been compared, for example, with results from microscopy (Bauer et al., 2008a) and culture samples (Chow et al., 2015b; Womiloju et al., 2003). Three organic molecules have been predominately utilized as unique tracers of fungal spores: ergosterol, mannitol, and arabitol. The majority of atmospherically relevant fungal spores are released by active wet discharge processes common in *Ascomycota* and *Basidiomycota*, meaning that the fungal organism actively ejects spores at a time most advantageous for the spore dispersal and germination processes, often when relative humidity (RH) is high (Ingold, 1971). While there are several mechanisms of active spore emission (e.g. Buller's drop (Buller, 1909) and osmotic pressure canons (Ingold, 1971)), they each involve the secretion of fluid containing hygroscopic compounds, such as arabitol, mannitol, potassium, chloride, and other solutes (Elbert et al., 2007), released near the site of spore growth. When the spores are ejected, some of the fluid adheres to the spores and becomes aerosolized. Several of these secreted compounds are thought to enter the atmosphere linked uniquely with spore emission processes, and so these tracers have been used to estimate atmospheric concentrations of fungal spores. Arabitol and mannitol are both sugar alcohols (polyols) that serve as energy stores for the spore (Feofilova, 2001). Arabitol is unique to fungal spores and lichen, while mannitol is present in fungal spores, lichen, algae, and higher plants (Lewis and Smith, 1967). Ergosterol is found within the cell membranes of fungal spores (Weete, 1973) and has been used as an ambient fungal spore trace (Di Filippo et al., 2013; Miller and Young, 1997). Comparing the seasonal trends of arabitol and mannitol with ergosterol, Burshtein et al. (2011) showed positive correlations between arabitol or mannitol and ergosterol only in the spring and autumn suggesting that the source of these polyols is unlikely to be solely fungal in origin or that the amount of each compound emitted varies considerably between species type and season. While ergosterol has been directly linked to fungal spores in the air, ergosterol is prone to photochemical degradation and is difficult to analyze and quantify directly. Quantification of ergosterol typically requires chemical derivatization by silylation before analysis via gas chromatography (Axelsson et al., 1995; Burshtein et al., 2011; Lau et al., 2006). In contrast, analysis of sugar alcohols by ion chromatography involves fewer steps and has been successfully applied to monitor seasonal variations of atmospheric aerosol concentration at a number of sites (Bauer et al., 2008a; Caseiro et al., 2007; Yang et al., 2012; Yttri et al., 2011a; Zhang et al., 2010; Zhang et al.,

98 2015) including pg m^{-3} levels in the Antarctic (Barbaro et al., 2015). By measuring spore count and tracer
99 concentration in parallel at one urban and two suburban sites in Vienna, Austria Bauer et al. (2008a)
100 estimated the amount of each tracer per fungal spore emitted. Potassium ions have also been linked to
101 emission of biogenic aerosol (Pöhlker et al., 2012b) and are co-emitted with fungal spores, however,
102 application of potassium as a fungal tracer is uncommon because it is predominantly associated with
103 biomass burning (Andreae and Crutzen, 1997). Additionally, (1→3)- β -D-glucan (fungal spores and
104 pollen) and endotoxins (gram-negative bacteria) have also been widely used to measure other bioaerosols
105 (Andreae and Crutzen, 1997; Cheng et al., 2012; Rathnayake et al., 2016b; Stone and Clarke, 1992).
106

107 The direct detection of PBAP has historically been limited to analysis techniques that require
108 culturing or microscopy of the samples. These systems are time-consuming, costly, and often
109 substantially undercount biological particles by an order of magnitude or more (Gonçalves et al., 2010;
110 Pyrri and Kapsanaki-Gotsi, 2007). The sampling methods associated with these measurements also offer
111 relatively low time resolution and low particle size resolution. Recently, techniques utilizing ultraviolet
112 laser/light-induced fluorescence (UV-LIF) for the real-time detection of PBAP have been developed and
113 are being utilized by the atmospheric community for bioaerosol detection. Thus far, the most widely
114 applied LIF instruments for ambient PBAP detection have been the Ultraviolet Aerosol Particle Sizer
115 (UV-APS; TSI Inc. Model 3314, St. Paul, MN) and the Wideband Integrated Bioaerosol Sensor (WIBS;
116 University of Hertfordshire, Hertfordshire, UK, now licensed to Droplet Measurement Technologies,
117 Boulder, CO, USA). Both of these commercially available instruments can provide information in real-
118 time about particle size and fluorescence properties of supermicron atmospheric aerosols.
119 Characterization and co-deployment of these instruments over the past ten years has expanded the
120 knowledge base regarding how to analyze and utilize the information provided from these instruments
121 (Crawford et al., 2015; Healy et al., 2014; Hernandez et al., 2016; Huffman et al., 2013; Perring et al.,
122 2015; Pöhlker et al., 2013; Pöhlker et al., 2012a; Ruske et al., 2016), though the interpretation of UV-LIF
123 results from individual particles is complicated by interfering material that is not biological in nature
124 (Gabey et al., 2010; Huffman et al., 2012; Lee et al., 2010; Saari et al., 2013; Toprak and Schnaiter,
125 2013).
126

127 Here we present analysis of atmospheric concentrations of arabitol and mannitol in relation to
128 results from real-time, ambient particle measurements reported by UV-APS and WIBS. We interrogate
129 these relationships as they pertain to rain conditions (rainfall and RH) that have previously been shown to
130 increase fluorescent aerosol concentration (Crawford et al., 2014; Huffman et al., 2013; Prenni et al.,
131 2013; Schumacher et al., 2013; Yue et al., 2016). Active wet discharge of ascospores and basidiospores
132 has frequently been reported to correspond with increased RH (Elbert et al., 2007), and fungal spore
133 concentration has also been shown to increase after rain events (e.g. Jones and Harrison, 2004). Here we
134 estimate airborne fungal concentrations in a semi-arid forest environment utilizing a combination of real-
135 time fluorescence methods, molecular fungal tracer methods, and direct-to-agar sampling and culturing as
136 parallel surrogates for spore analysis. This study of ambient aerosol represents the first ambient
137 quantitative comparison of real-time aerosol UV-LIF instruments with results from molecular tracers or
138 culturing.
139

140 2. Methods

141 2.1 Sampling site

142 Atmospheric sampling was conducted as a part of the BEACHON-RoMBAS (Bio-hydro-
143 atmosphere interactions of Energy, Aerosols, Carbon, H_2O , Organics, and Nitrogen – Rocky Mountain
144 Biogenic Aerosol Study) field campaign conducted at the Manitou Experimental Forest Observatory
145 (MEFO) located 48 km northwest of Colorado Springs, Colorado (2370 m elevation, 39° 06' 0" N, 105°
146 5' 03" W) (Ortega et al., 2014). The site is located in the central Rocky Mountains and is representative of
147 semi-arid montane pine forested regions of North America. During BEACHON-RoMBAS, a large team
148

149 of, international team of researchers conducted an intensive set of measurements from 20 July to 23
150 August 2011. A summary of results from the campaign are published in the BEACHON campaign special
151 issue of Atmospheric Chemistry and Physics¹. All the data used in this study reported here were gathered
152 from instruments and sensors located within a <100 m radius (e.g. Fig. 1).

153

154 2.2 Online fluorescent instruments

155 A UV-APS and WIBS-3 (Model 3; University of Hertfordshire) were operated continuously as a
156 part of the study, and particle data were integrated to five-minute averages before further analysis. The
157 UV-APS was operated under procedures defined in previous studies (Huffman et al., 2013; Schumacher
158 et al., 2013). A total suspended particle (TSP) inlet head ~5.5 m above ground, mounted above the roof of
159 a climate-controlled, metal trailer, was used to sample aerosol directed towards the UV-APS. Bends and
160 horizontal stretches in the 0.75 inch tubing were minimized to reduce losses of large particles (Huffman et
161 al., 2013). The UV-APS detects particles between 0.5-20 μm and records aerodynamic particle diameter
162 and integrated total fluorescence (420-575 nm) after pulsed excitation by a 355 nm laser (Hairston et al.,
163 1997). Both UV-APS and WIBS instruments report information about particle number concentration, but
164 it is instructive here to show results in particle mass for comparison between all techniques. Total particle
165 number size distributions (irrespective of fluorescence properties) obtained from the UV-APS and WIBS
166 were converted to mass distributions using assuming spherical particles of unit particle mass density of as
167 a first approximation for all direct comparisons with tracer mass and, unless otherwise stated. Total
168 particle concentration values (in $\mu\text{g m}^{-3}$) were obtained for each five-minute period by integrating over the
169 size range 0.5 – 15 μm , and these mass concentration values were averaged over the length of the filter
170 sampling periods. Uncertainty in mass concentration values reported here is influenced by utilizing a
171 single, estimated value for particle mass density and because of slight dissimilarities between UV-APS
172 and WIBS instruments in size binning at particle sizes above 10 μm that dominate particle mass.

173

174 A WIBS-3 was used to continuously sample air at a site ~50 m away from the UV-APS trailer
175 and 1.3 m above the ground. Briefly, the diameter of individual particles sampled by the WIBS is
176 estimated by the intensity of the elastic side-scatter from a continuous wave 635 nm diode laser and
177 analyzed by a Mie scattering model (Foot et al., 2008; Kaye et al., 2005). Particles that pass through the
178 diode laser activate two optically-filtered Xenon flash lamps. The first lamp excites the particle at 280 nm
179 and the second at 370 nm. Emission from the 280 nm excitation is filtered separately for two PMTs, one
180 which detects in a band at 310 320-400 nm and the other in a band at 410-650 nm. These excitation and
181 emission wavelengths result in a total of three channels of detection: λ_{ex} 280 nm, λ_{em} 320 – 400 nm (FL 1
182 or Channel A); λ_{ex} 280 nm, λ_{em} 410 – 650 nm (FL 2 or Channel B); and λ_{ex} 370 nm, λ_{em} 410– 650 nm (FL
183 3 or Channel C) (Crawford et al., 2015). Individual particles are considered fluorescent here if they
184 exceed fluorescent thresholds for any channel, as defined as the average of a “forced trigger” baseline
185 plus 3 standard deviations (σ) of the baseline measurement (Gabey et al., 2010).

186

187 WIBS particle-type analysis is utilized to define types of particles that have specific spectral
188 patterns. As defined by Perring et al. (2015), the 3 different fluorescent channels (FL1, FL2, and FL3) can
189 be combined to produce 7 unique fluorescent categories. Observed fluorescence in channel FL1 alone, but
190 without any detectable fluorescence in Channel FL2 or FL3, categorizes a particle as type A. Similarly,
191 observed fluorescence in channels FL2 or FL3, but in no other channels, places a particle in the B or C
192 categories, respectively. Combinations of fluorescence in these channels, such as a particle that exhibits
193 fluorescence in both FL1 and FL2 categorizes a particle as type AB and so on for a possible seven particle
194 types as summarized in Figure S1.

195

¹http://www.atmos-chem-phys.net/special_issue247.html

196 As a separate tool for particle categorization, the University of Manchester has recently developed and
197 applied a hierarchical agglomerative cluster analysis tool for WIBS data, which they have **previously**
198 applied to the BEACHON-RoMBAS campaign (Crawford et al., 2014; Crawford et al., 2015; Robinson et
199 al., 2013). Here we utilize clusters derived from WIBS-3 data as described by Crawford et al. (2015).
200 Cluster data presented here was analyzed with the Open Source Python package FastCluster (Mullner,
201 2013). Briefly, hierarchical agglomerative cluster analysis was applied to the entire data set and each
202 fluorescent particle was uniquely clustered into one of 4 groups. Cluster 1, assigned by Crawford et al.
203 (2015) as fungal spores, displayed a 1.5-2 μm mode and a daily peak in the early morning that paralleled
204 relative humidity (Schumacher et al., 2013). Clusters 2, 3, and 4 have strong, positive correlations with
205 rainfall and exhibit size modes that peak at $<1.2 \mu\text{m}$ and were initially described by Crawford et al. as
206 bacterial particles. Here we have summed Clusters 2-4 to a single group referred to as Cl_{Bact} , for
207 simplicity when comparing with molecular tracers. **It should be noted that assignment of name and origin**
208 **(e.g. fungal spores or bacteria) to clusters is approximate and does not imply particle homogeneity. Each**
209 **cluster likely contains an unknown fraction of contaminating particles, but the clusters are beneficial to**
210 **group particles more selectively than using fluorescent intensity alone. For more details see Robinson et**
211 **al. (2013) and Crawford et al. (2015).**

212
213 The WIBS-3 utilized here has since **been updated to been superseded by** the WIBS-4 (Univ.
214 Hertfordshire, UK) and WIBS-4A (Droplet Measurement Technologies, Boulder, Colorado). One
215 important difference between the models is that the **WIBS-3 exhibits comparatively weak FL1 and FL2**
216 **signals with respect to the more updated models, and is thus more influenced by FL3. This results in a**
217 **different break-down of** optical chamber design and filters of the WIBS-4 models were updated to
218 enhance the overall sensitivity of the instrument (Crawford et al., 2014). Additionally, **slight differences**
219 **in detector gain between models and individual units can impact the relative sensitivity of the**
220 **fluorescence channels. . This may result in differences in fluorescent** channel intensity between
221 instrument models, as will be discussed later.

222 223 **2.3 High volume sampler**

224 Total suspended particle samples were collected for molecular tracer and molecular genetic
225 analyses using a high volume sampler (Digitel DHA-80) drawing 1000 L min^{-1} through 15 cm glass fiber
226 filters (Macherey-Nagel GmbH, Type MN 85/90, 406015, Düren, Germany) over a variety of sampling
227 times ranging from 4-48 h (supplemental Table S1). The sampler was located $<50 \text{ m}$ from each of the
228 UV-LIF instruments described here, approximately between the WIBS-3 and UV-APS. Prior to sampling
229 all filters were baked at $500 \text{ }^\circ\text{C}$ for 12 h to remove DNA and organic contaminants. Samples were stored
230 in pre-baked aluminum bags after sampling at $-20 \text{ }^\circ\text{C}$ for 1-30 days and then at $-80 \text{ }^\circ\text{C}$ after overnight,
231 international transport cooled on dry ice. Due to the low vapor pressure of the molecular tracers analyzed
232 loss due to volatilization is considered unlikely (Zhang et al., 2010). 36 samples were collected during the
233 study, in addition to handling field blanks and operational field blanks. Handling blanks were acquired by
234 placing a filter into the sampler and immediately removing, without turning on the air flow control.
235 Operational blanks were placed into the sampler and exposed to 10 seconds of air flow.

236 237 **2.4 Slit Sampler**

238 A direct-to-agar slit sampler (Microbiological Air Sampler STA-203, New Brunswick Scientific
239 Co, Inc., Edison, NJ) was used to collect culturable airborne fungal spores. The sampler was placed $\sim 2 \text{ m}$
240 above ground on a wooden support surface with 5 cm x 5 cm holes to allow air flow both up and down
241 through the support structure. Sampled air was drawn over the 15 cm diameter sampling plate filled with
242 growth media at a flow rate of 28 L min^{-1} for sampling periods of 20 to 40 min. Growth media (malt
243 extract medium) was mixed with antibacterial agents (40 units streptomycin, Sigma Aldrich; 20 units
244 ampicillin, Fisher Scientific) to suppress bacterial colony growth. Plates were prepared several weeks in
245 advance and stored in a refrigerator at ca. $4 \text{ }^\circ\text{C}$ until used for sampling. Before each sampling period, all
246 surfaces of the samplers were sterilized by wiping with isopropyl alcohol. Handling and operational

247 blanks were collected to verify that no fungal colonies were being introduced by handling procedures. 14
248 air samples were collected over 20 days and immediately moved to an incubator (Amerex Instruments,
249 Incumax IC150R) set at 25 °C for 3 days prior to counting fungal colonies formed. Each colony, present
250 as a growing dot on the agar surface, is assumed to have originated as one colony forming unit (CFU; i.e.
251 fungal spore) deposited onto the agar by impaction during sampling. The atmospheric concentration of
252 CFU per air volume was calculated using the sampler air flow. Further discussion of methods and initial
253 results from the slit sampler were published by Huffman et al. (2013).

254

255 **2.5 Offline filter analyses**

256

257 *2.5.1 Carbohydrate analysis*

258 Approximately 1/8 of each frozen filter was cut for carbohydrate analysis using a sterile
259 technique, meaning that scissors were cleaned and sterilized and cutting was performed in a positive-
260 pressure laminar flow hood. In order to precisely determine the fractional area of the filter to be analyzed,
261 filters were imaged from a fixed distance above using a camera and compared to a whole, intact filter.
262 Using ImageJ software (Rasband and ImageJ, 1997), the area of each filter slice showing particulate
263 matter (PM) deposit was referenced to a whole filter, and thereby the amount of each filter utilized could
264 be determined. **This** The total PM mass was not measured and so this technique allowed for an estimate
265 estimation of the fraction of each sampled used for the analysis, which corresponds to the fraction of PM
266 mass deposited. The uncertainty on the filter area fraction is estimated at 2%. The uncertainty was
267 determined as the percent of variation in the area of the filter edge (no PM deposit) as compared to the
268 total filter area.

269

270 **Water soluble** carbohydrates were extracted from quartz filter samples and analyzed following the
271 procedure described by Rathnayake et al. (2016a). A total of 36 samples were analyzed along with field
272 and lab blanks. All lab and field blanks fell below method detection limits. Extraction was performed by
273 placing the filter slice into a centrifuge tube that had been pre-rinsed with Nanopure™ water (resistance >
274 18.2 MΩ cm⁻¹; Barnstead EasyPure II, 7401). A volume of 8.0 mL of Nanopure™ water was added to the
275 filter in the centrifuge tube to extract water-soluble carbohydrates. Samples were then exposed to rotary
276 shaking for 10 min at 125 rpm, sonication for 30 min at 60 Hz (Branson 5510, Danbury, CT, US), and
277 rotary shaking for **another** 10 min. After shaking, the extracted solutions were filtered through a 0.45 μm
278 polypropylene syringe filter (GE Healthcare, UK) to remove insoluble particles, including disintegrated
279 filter pieces. One 1.5 mL aliquot of each extracted solution was analyzed for carbohydrates within 24
280 hours of extraction. A duplicate 1.5 mL aliquot was stored in a freezer and analyzed, if necessary due to
281 lack of instrument response and invalid calibration check, within 7 days of extraction. Analysis of
282 carbohydrates was done using a High Performance Anion Exchange Chromatography System with Pulsed
283 Amperometric Detection (HPAEC-PAD, Dionex ICS 5000, Thermo Fisher, Sunnyvale, CA, USA).
284 Details of the instrument specifications and quality standards for carbohydrate determination are available
285 in Rathnayake et al. (2016). Calibration curves for mannitol, levoglucosan, glucose (Sigma-Aldrich),
286 arabitol and erythritol (Alfa Aesar) were generated with seven points each, ranging in aqueous
287 concentration from 0.005 ppm to 5 ppm. The method detection limits for mannitol, levoglucosan, glucose,
288 arabitol, and erythritol were 2.3, 2.8, 1.6, 1.0, and 0.6 ppb, respectively. Method detection limits were
289 determined as 3σ of analyte concentrations recovered from seven spiked filter samples (Rathnayake et al.,
290 2016a). All calibration curves were checked daily using a standard solution to ensure all concentration
291 values were within 10% of the known value. Failure to maintain a valid curve resulted in recalibration of
292 the instrument.

293

294 *2.5.2 DNA analysis*

295 Methods and initial results from DNA analysis from these high volume filters were published by
296 Huffman et al. (2013). Briefly, fungal diversity was determined by previously optimized methods for
297 DNA extraction, amplification, and sequence analysis of the internal transcribed spacer regions of

298 ribosomal genes from the high volume filter samples (Fröhlich-Nowoisky et al., 2012; Fröhlich-
299 Nowoisky et al., 2009). Upon sequence determination, fungal sequences were compared with known
300 sequences using the Basic Local Alignment Search Tool (BLAST) at the National Center for
301 Biotechnology (NCBI) and identified to the lowest taxonomic rank common to the top BLAST hits after
302 chimeric sequences had been removed. When sequences displayed >97% similarity, they were grouped
303 into operational taxonomic units (OTUs).

304 305 2.5.3 Endotoxin and glucan analysis

306 Sample preparation for quantification of endotoxin and (1→3)-β-D-glucan included extraction of
307 5 punches (0.5 cm² each) of the quartz filters with 5.0 mL of pyrogen-free water (Associates of Cape Cod
308 Inc., East Falmouth, MA, USA), utilizing an orbital shaker (300 rpm) at room temperature for 60 min,
309 followed by centrifuging for 15 min (1000 rpm). One-half mL of supernatant was submitted to a kinetic
310 chromogenic limulus amoebocyte lysate (Chromo-LAL) endotoxin assay (Associates of Cape Cod Inc.,
311 East Falmouth, MA, USA) using a ELx808IU (BioTek Instrument Inc., Winooski, VT, USA) incubating
312 absorbance microplate reader. For (1→3)-β-D-glucan measurement, 0.5 mL of 3 N NaOH was added to
313 the remaining 4.5 mL of extract and the mixture was agitated for 60 min. Subsequently, the solution was
314 neutralized to pH 6–8 by addition of 0.75 mL of 2 N HCl. After centrifuging for 15 min (1→3)-β-D-
315 glucan concentration was determined in the supernatant using the GlucateLL® LAL kinetic assay
316 (Associates of Cape Cod, Inc., East Falmouth, MA). The minimum detection limits (MDLs) and
317 reproducibility were 0.046 Endotoxin Units (EU) m⁻³ and ± 6.4% for endotoxin and 0.029 ng m⁻³ and ±
318 4.2% for (1→3)-β-D-glucan, respectively. Laboratory and field blank samples were analyzed as well,
319 with lab blank values being below detection limits, while field blank values were used to subtract
320 background levels from sample data. More details about the bioassays can be found elsewhere (Chow et
321 al., 2015a).

322 323 2.6 Meteorology and wetness sensors

324 Meteorological data were recorded by a variety of sensors located at the site. Precipitation was recorded
325 by a laser optical disdrometer (PARTicle SIze and VELOCITY “PARSIVEL” sensor; OTT Hydromet
326 GmbH, Kempten, Germany) and separately by a tipping bucket rain gauge. The disdrometer provides
327 precipitation occurrence, rate, and physical state (rain or hail) by measuring the magnitude and duration
328 of disruption to a continuous 780 nm laser that was located in a tree clearing (Fig. 1), while the tipping
329 bucket rain gauge measures a set amount of precipitation before tipping and triggering an electrical pulse.
330 A leaf wetness sensor (LWS; Decagon Devices, Inc., Pullman, WA), provided a measurement of
331 condensed moisture by measuring the voltage drop across a leaf surface to determine a proportional
332 amount of water on or near the sensor. Additional details of these measurements can be found in Huffman
333 et al. (2013) and Ortega et al. (2014).

334 335 3. Results and Discussion

336 337 3.1 Categorization and characteristic differences of Dry and Rainy periods

338 Increases in PBAP concentration have been frequently associated with rainfall (e.g. Bigg et al.,
339 2015; Faulwetter, 1917; Hirst and Stedman, 1963; Jones and Harrison, 2004; Madden, 1997). Fungal
340 polyols have also been reported to increase after rain and have been used as indicators of increased fungal
341 spore release (Liang et al., 2013; Lin and Li, 2000; Zhu et al., 2015). Recently it was shown that the
342 concentration of fluorescent aerosol particles (FAP) measured during BEACHON-RoMBAS increased
343 dramatically during and after periods of rain (Crawford et al., 2014; Huffman et al., 2013; Schumacher et
344 al., 2013) and that these particles were associated with high concentrations of ice nucleating particles that
345 could influence the formation and evolution of mixed-phase clouds (Huffman et al., 2013; Prenni et al.,
346 2013; Tobo et al., 2013). It was observed that a mode of smaller fluorescent particles (2-3 μm) appeared
347 during rain episodes, and several hours after rain ceased a second mode of slightly larger fluorescent
348 particle (4-6 μm) emerged, persisting for up to 12 h (Huffman et al., 2013). The first mode was

349 hypothesized to result from mechanical ejection of particles due to rain splash on soil and vegetated
350 surfaces, and the second mode was suggested as actively emitted fungal spores (Huffman et al., 2013).
351 While the UV-APS and WIBS each provide data at high enough time resolution to see subtle changes in
352 aerosol concentration, the temporal resolution of the chemical tracer analysis was limited to 4-48 h
353 periods defined by the collection time of the high volume sampler. To compare the measurement results
354 across the sampling platforms, UV-LIF measurements were averaged to the lower time resolution of the
355 filter sampler periods, and the periods were grouped into three broad categories: Rainy, Dry, and Other, as
356 will be defined below.

357 Time periods were wetness-categorized in two steps: first at 15 min resolution and then averaged
358 for each individual filter sample. During the first stage of categorization each 15 min period was
359 categorized into one of four groups: rain, post-rain, dry, or other. To categorize each filter period, an
360 algorithm was established utilizing UV-APS fluorescent particle fraction and accumulated rainfall. The
361 ratio of integrated number of fluorescent particles to total particles was used as a proxy for the increased
362 emission of biological particles. Figure 2a presents a time series of the size-resolved fluorescent particle
363 concentration, showing increases during rain periods in dark red. A relatively consistent diurnal cycle of
364 increased FAP concentration in the 2-4 μm range is apparent almost every afternoon, which corresponds
365 to near daily afternoon rainfall during approximately the first half of the measurement period.
366 Disdrometer and tipping bucket rainfall measurements were each normalized to unity and summed to
367 produce a more robust measure of rainfall rate, because it was observed that often only one of the two
368 systems would record a given light rain event. If a point was described by total rainfall accumulation
369 greater than 0.201 it was flagged as rain. A point was flagged as post-rain if it immediately followed a
370 rain period and also exhibited a fluorescent particle fraction greater than 0.08. The purpose of this
371 category was to reflect the observation that sustained, elevated concentrations of FAP persisted for many
372 hours even after the rain rate, RH, and leaf wetness returned to pre-rain values. The only measurement
373 that adequately reflected this scenario was of the fluorescent particles measured by UV-APS and WIBS
374 instruments. The post-rain flag was continued until the fluorescent particle fraction fell below 0.08 or if it
375 started to rain again (with calculated rain values greater than 0.201). Points were flagged as dry periods if
376 they exhibited rainfall accumulation and fluorescent particle fraction below the thresholds stated above.
377 Several periods were not easily categorized by this system and were considered in a fourth category as
378 other. This occurred when fluorescent particle fraction above the threshold value was observed with no
379 discernable rainfall.

380
381 Once wetness categories were assigned by the algorithm at 15 min resolution, each high volume
382 filter sample was categorized by a similar nomenclature, but using only three categories. These were
383 defined as Dry, Rainy (combination of rain and post rain categories), or Other based on the relative time
384 fraction in each of the four original 15 min categories. For each sample, if the relative time fraction of a
385 given category exceeded 0.50 the sample was assigned to that category. Despite the effort to categorize
386 samples systematically, several sample periods (5 of 35) appeared mis-categorized by looking at FAP
387 concentration, rainfall, RH, and leaf wetness in more detail. In some circumstances, this was because light
388 rainfall produced observable increases in FAP, but without exceeding the rainfall threshold. Or in other
389 circumstances a period of rainfall occurred at the very end or just before the beginning of a sample, and so
390 the many-hour period was heavily influenced by aerosol triggered by a period of rain just outside of the
391 sample time window. As a result, several samples were manually re-categorized as described here.
392 Samples 20 and 21 (Table S1) were four-hour samples that displayed high relative humidity and rainfall,
393 thus samples were originally characterized as Rainy. This period was described by an extremely heavy
394 rain downpour (7.5 mm in 15 min), however, that seemingly placed the samples in a different regime of
395 rain-aerosol dynamics than the other Rainy samples and so these two samples were moved to the Other
396 category. Sample 23, originally Rainy, presented a FAP fraction marginally above the 0.08 threshold, but
397 visually displayed a trend dissimilar to other post-rain periods and so was re-categorized as Dry. Sample
398 28 showed no obvious rainfall, but the measurement team observed persistent fog in three consecutive
399 mornings (Samples 25, 27, 28), and the concentration of fluorescent particles (2-6 μm) suggested a source

400 of particles not influenced by rain, and so this Rainy sample was re-categorized as Other. Sample 38
401 displayed a fluorescent number ratio just below the threshold value, and was **thus first** categorized as Dry,
402 however, the measurement team observed post-rain periods at the beginning and end of the sample, so the
403 sample were re-categorized as Other. For all samples other than these five, the categorization was
404 determined using the majority (> 0.50) of the 15 min periods. In no cases other than the five that were re-
405 categorized was the highest category fraction less than 0.50 of the sample time. Note that we have chosen
406 to capitalize Rainy, Dry, and Other to highlight that we have rigorously defined the period using the
407 characterization scheme described above and to separate the nomenclature from the general, colloquial
408 usage of the terms. Wetness category assignment for each high volume filter sample period is shown in
409 Figure 2 as a background color (brown for Dry samples, green for Rain-influenced samples, and pink for
410 Other samples) and Table S1.

411
412 To validate the qualitative differences between wetness categories described in the last section,
413 we present observations about each of these groupings. First, we organized the WIBS data according to
414 the particle categories introduced by Perring et al. (2015). By this method, every fluorescent particle
415 detected by the WIBS can be defined uniquely into one of seven categories (i.e. A, AB, ABC and so on).
416 By plotting the relative fraction of fluorescent particles described by each particle type, temporal
417 differences between measurement periods can be observed, as shown in Figure 2e. To a first
418 approximation, this analysis style allows for coarse discrimination of particle types. For example, a given
419 population of particles would ideally exhibit a consistent fraction of particles present in the different
420 particle categories as a function of time. By this reasoning, sample periods categorized as Dry (most of
421 the latter half of the study; brown bars in Fig. 2) would be expected to have a self-consistent particle type
422 trend, whereas sample periods categorized as Rainy (most of the first half of the study; green bars in Fig.
423 2) would have a self-consistent particle type trend, but different from the Dry samples. This is broadly
424 true. During Rainy periods as seen in Figure 3a, there is a relatively high fraction ($> 65\%$) of ABC
425 particles (light blue) and a relatively low fraction ($< 15\%$) in BC (purple) and C (yellow) type particles,
426 suggesting heavy influence from the FL1 channel. In contrast, during Dry periods the fraction of ABC
427 particles (light blue) is reduced ($< 25\%$) while BC (purple) and C (yellow) type particles increase in
428 relative fraction ($> 30\%$ and $> 40\%$, respectively) suggested a diminished influence of FL1 channel.

429
430 It is important to note a few important caveats here. First, the ability of the WIBS to discriminate
431 finely between PBAP types is relatively poor and it is still unclear exactly how different particle types
432 would appear by this analysis method. Particles of different kinds and from different sources are likely
433 convolved into a single WIBS particle type, which could either soften or enhance the relationships with
434 rain discussed here. Second, the assignment of particle types is heavily size-dependent and sensitive to
435 subtle instrument parameters, and so it is unclear how different instruments would present similar particle
436 types. For example, Hernandez et al. (2016) used two WIBS instruments and found differences in relative
437 fraction of particle categories for samples aerosolized in the lab. They reported fungal spores to be
438 predominately A, AB, and ABC type particles, whereas Rainy sample periods suggested to have heavy
439 fungal spore influence by Huffman et al. (2013) show predominantly C, BC, and ABC particle fraction.
440 These discrepancies may be due to the comparison of ambient particles to laboratory-grown cultures. The
441 highly controlled environment of a laboratory may not always accurately represent the humidity
442 conditions in which fungal spore release occurs in this forest setting (Saari et al., 2015). This **would**
443 **impact the fluorescence properties of fungal spore particles which are inhibited by increased moisture**
444 **level around the spore that have differing amounts of adsorbed or associated water** (Hill et al., 2009,
445 2013, 2015). More likely, however, is that the WIBS-3 used here exhibits **higher differences in** sensitivity
446 **in the FL3 channel with respect to the FL1 and FL2 channels** (Robinson et al., 2013), as compared to
447 **from the WIBS-4A used as one of the units reported by Hernandez et al. (2016). This would Even a slight**
448 **increase in sensitivity in the FL3 channel with respect to the FL1 or FL2 channels could** explain the shift
449 here towards particles with C-type fluorescence. One piece of evidence for this is the quantitative
450 comparison of particle measurements presented by the UV-APS and WIBS-3 instruments co-deployed

451 here (Fig. 4). The number concentration of particle exhibiting fluorescence above the FL2 baseline of the
452 WIBS-3 is approximately consistent with the number of fluorescent particles measured by the UV-APS,
453 and significantly below the concentration of FL3 particles. The UV-APS number concentration shows the
454 highest correlation with the WIBS-3 FL2 channel: during Rainy periods, $R^2=0.70$; Dry, $R^2=0.82$; Other,
455 $R^2=0.92$. These observations are in stark contrast to the trends reported by Healy et al. (2014) that the
456 UV-APS fluorescent particle concentration correlated most strongly with the WIBS-4 FL3 and that the
457 number concentration of FL3 was the lowest out of all three channels. Given that the FL3 channel of the
458 WIBS and the UV-APS probe cover similar excitation and emission wavelengths it is expected that these
459 two channels should correlate well. Based on these data, we suggest that the WIBS-3 utilized here may
460 present a very different particle type break-down than if a WIBS-4 had been used. So, while caution is
461 recommended when comparing the relative break-down of WIBS particle categories shown here (Fig. 3)
462 with other studies, the data are internally self-consistent, and comparing qualitative differences between,
463 e.g. Rainy and Dry periods is expected to be robust. The main point to be highlighted here is that there is
464 indeed a qualitative difference in particles present in the three wetness categories, as averaged and shown
465 in Figure 3a, which generally supports the effort to segregate these samples.
466

467 Further evidence that there is a qualitative difference in the three wetness categories is shown
468 using molecular genetic analysis (Figs. 3b, c). The analysis of fungal DNA sequences from 21 of the high
469 volume samples found 406 operational taxonomic units (OTUs), belonging to different fungal classes and
470 phyla. When organized by wetness type it was observed that 106 of these occurred only on Rainy
471 samples, 148 of these occurred on Dry samples, and 37 on Other samples, with some fraction occurring in
472 overlaps of each (Fig. 3c). This shows that the number of OTUs observed uniquely in either the Rainy or
473 Dry periods is greater than the number of OTUs present in both wetness types, suggesting that the fungal
474 communities in each grouping are relatively distinct. Further, Figure 3b shows a break-down of fungal
475 taxonomic groupings for each wetness group. This analysis shows that there is a qualitative difference in
476 taxonomic break-down between periods of Rainy and Dry. Specifically, during Dry periods there is an
477 increased fraction of Pucciniomycetes (green bar, Fig. 3c), Chytridiomycota (yellow), Sordariomycetes
478 (orange), and Eurotiomycetes (pink) when compared to the Rainy periods.
479

480 3.2 Atmospheric mass concentration of arabitol, mannitol, and fungal spores

481 To estimate fungal spore emission to the atmosphere, the concentration of arabitol and mannitol
482 (Fig. 5a, b, Table S2) in each aerosol sample was averaged for all samples in each of the three wetness
483 categories. The average TSP-concentration of arabitol collected on Dry samples increased by a factor of
484 3.3 on Rainy TSP samples ($35.2 \pm 10.5 \text{ ng m}^{-3}$) increased by a factor of 3.3 with respect to Dry samples,
485 and the average TSP mannitol concentration on Rainy samples was higher by a factor of 3.7 (44.9 ± 13.8
486 ng m^{-3}). Figures 5a, b show the concentration variability for each wetness category, observed as the
487 standard deviation from the distribution of individual samples. For each polyol, there is no overlap in the
488 ranges shown, including the outliers of the Rainy and Dry category, suggesting a definitive and
489 conceptually distinct separation between dry periods and those influenced by rain. The concentrations
490 observed during Other periods is between those of the Dry and Rainy averages, as expected, given the
491 difficulty in confidently assigning these uniquely to one of these categories. The observations here are
492 roughly consistent with previous reports of polyol concentration, despite differences in local fungal
493 communities and concentrations. For example, Rathnayake et al. (2016a) observed 30.2 ng m^{-3} arabitol
494 and 41.3 ng m^{-3} mannitol in PM_{10} samples collected in rural Iowa, USA. In addition, Zhang et al. (2015)
495 reported arabitol and mannitol concentrations in PM_{10} samples of 44.0 and 71.0 ng m^{-3} , respectively, from
496 a study in the mountains on Hainan Island off the coast of Southern China. More recently, Yue et al.
497 (2016) studied a rain event in Beijing and observed increased polyol concentrations at the onset of the
498 rain. The observed mannitol concentration (45 ng m^{-3}) was approximately consistent with observations
499 reported here and with previous reports, while the arabitol concentration values observed were
500 approximately an order of magnitude lower (0.3 ng m^{-3}).
501

502 The square of the correlation coefficient (R^2) here between concentration values of arabitol and
503 mannitol during Rainy samples is very high (0.839; Table 1) suggesting that arabitol and mannitol
504 originated primarily from the same source, likely active-discharge fungal spores. The correlation is
505 similar to the 0.87 R^2 reported by Bauer et al. (2008a) and the 0.93 R^2 reported by Graham et al. (2003).
506 In contrast, the same correlation between mannitol and arabitol concentrations, but for Dry samples is
507 relatively low (0.312). This is consistent with reports that arabitol can be used more specifically as a spore
508 tracer, but that mannitol has additional atmospheric sources besides fungal spores. The same correlation
509 was also performed between arabitol or mannitol and other molecular tracers (endotoxins and (1→3)- β -
510 D-glucan), but all R^2 value were less than 0.43, suggesting that the endotoxins and glucans analyzed were
511 not emitted uniquely from the same sources as arabitol and mannitol.

512
513 Results from the two UV-LIF instruments were averaged over high volume sample periods, and a
514 correlation analysis was performed between tracer mass and fluorescent particle mass showing positive
515 correlations in all cases. The FAP mass from the UV-APS shows high correlation with the fungal polyols
516 during Rainy periods, with R^2 of 0.732 and 0.877 for arabitol and mannitol, respectively (Table 2; Figure
517 5c, d). The same tracers correlate poorly with the UV-LIF during Dry conditions. This is expected,
518 because polyols such as arabitol and mannitol are only found in *Ascomycota* and *Basidiomycota* fungal
519 spores which both utilize ascomycetes and basidiomycetes emitted by wet discharge methods are the only
520 fungal spores associated with arabitol and mannitol. for spore dispersal (Elbert et al., 2007; Feofilova,
521 2001; Lewis and Smith, 1967). This high correlation suggests that the UV-APS does a good job of
522 detecting these wet-discharge spores, and corroborates previous statements that particles detected by the
523 UV-APS are often predominately fungal spores (Healy et al., 2014; Huffman et al., 2013; Huffman et al.,
524 2012). In contrast, the low slope value and the poor correlation during Dry periods suggest that the UV-
525 APS is also sensitive to other kinds of particles, as designed. The small positive x-offset (FAP mass;
526 Table S2, Figs. 5c,d) during Rainy periods is likely due to particles that are too weakly fluorescent to be
527 detected and counted by the UV-APS, which is consistent with observations made in Brazil (Huffman et
528 al., 2012).

529
530 Particle mass from WIBS C11, assigned to fungal spores (Crawford et al., 2015), also correlated
531 strongly with the same two molecular tracers. Both Rainy periods (R^2 0.824) and Dry periods (R^2 0.764)
532 correlate well with arabitol (Fig. 5e), while mannitol (Fig. 5f) only shows a strong correlation during the
533 Rainy periods (R^2 0.799). Mannitol is a common polyol in higher plants while arabitol is only found in
534 fungal spores and lichen (Lewis and Smith, 1967). So the strong correlation of each polyol with UV-LIF
535 mass during Rainy periods when actively-discharged spores are expected to dominate and the similarly
536 strong correlations associated with arabitol suggest that the C11 cluster does a reasonably good job of
537 selecting fungal spore particles. The poor correlation between mannitol and C11 during dry periods
538 illustrates that the background mannitol concentration is likely not due to fungal spores alone, but has
539 contribution from other higher plants that contain mannitol. Particle concentrations detected by individual
540 WIBS channels and in the other cluster were also compared with polyol concentrations, but each
541 correlation is relatively poor compared to that with respect to C11. As seen in Table 2 and Figures S2-S3,
542 correlations in FL1, 2, and 3 with arabitol are poor (<0.4) in the Dry category and good ($0.4 < R^2 < 0.7$) in
543 the Rainy category. For mannitol, all the UV-LIF instruments show high correlation (>0.7) in all cases.
544 This is likely due to mannitol being a non-specific tracer and suggests that the majority of UV-LIF
545 particles observed during all periods was dominated by PBAP.

546 3.3 Estimated number concentration of fungal spore aerosol

547
548 Bauer et al. (2008a) reported measurements of fungal spore number concentration in Vienna,
549 Austria using epifluorescence microscopy and also measured fungal tracer mass concentrations collected
550 onto filters in order to estimate the mass of arabitol (1.2 to 2.4 pg spore^{-1}) and mannitol (0.8 to 1.8 pg
551 spore^{-1}) associated with each emitted spore. Bauer et al. (2008a) and (Yttri et al., 2011b) reported ratios of
552 mannitol to arabitol of approximately 1.5 (\pm standard deviation of 26%) and 1.4 ± 0.3 , respectively. Our

553 measurements show slightly lower ratios of mannitol to arabitol, but that the ratio is dependent on
554 wetness category; Rainy, 1.29 ± 0.17 ; Dry, 1.12 ± 0.23 ; and Other, 1.24 ± 0.54 . The mannitol to arabitol
555 ratio would be expected to vary as a function of fungal population present in the aerosol, whether between
556 different wetness periods at a given location or between different physical localities.

557
558 Using the approximate mid-point of the Bauer et al. (2008a) reported ranges, 1.7 pg mannitol per
559 spore and 1.2 pg arabitol per spore, atmospheric number concentrations of spores collected onto the high
560 volume filters were calculated from the polyol mass concentrations measured here. Based on these values,
561 and assuming all polyol mass originated with spore release, the mass concentration averages (Fig. 5) were
562 converted to fungal spore number concentrations (Fig. 6). The trends of spore concentration averages are
563 the same as with the polyol mass, because the numbers were each multiplied by the same scalar value.
564 After doing so, the analysis reveals an estimated spore concentration during Dry periods of 0.89×10^4 (\pm
565 0.21) spores m^{-3} using the arabitol concentration and 0.70×10^4 (± 0.19) spores m^{-3} using the mannitol
566 concentration (Table 3). The estimated concentration of spores increased approximately three-fold during
567 Rainy periods to 2.9×10^4 (± 0.8) spores m^{-3} (arabitol estimate) and 2.6×10^4 (± 0.8) spores m^{-3} (mannitol
568 estimate) (Figure 6a, b). These estimates match well with estimates reported by Spracklen and Heald
569 (2014), who modeled the concentration of airborne fungal spores across the globe as an average of $2.5 \times$
570 10^4 spores m^{-3} , with approximately 0.5×10^4 spores m^{-3} over Colorado.

571
572 The UV-LIF instruments discussed here are fundamentally number-counting techniques and in
573 this instance have been applied can be utilized roughly as spore counters. As a first approximation, each
574 particle detected by the UV-APS was assumed to be a fungal spore with the same properties used in the
575 assumptions by Bauer et al. (2008a). Figures 6d,e,g,h show correlations Plotting the correlation of fungal
576 spore number concentration estimated from polyol mass on the y-axis concentration with respect to the
577 fungal spore concentration assumed from the UV-LIF measurements on the x-axis. shows correlations in
578 Figures 6e,d-f. The first, and most important observation is that the estimated fungal spore concentration
579 from each technique is on the same order of magnitude, $10^4 m^{-3}$. Looking at individual correlations
580 reveals a finer layer of detail. These results show that the number concentration of fungal spores
581 estimated by the UV-APS is greater than the number of fungal spores estimated by the tracers, as
582 evidenced by slope values of approximately 0.2 and 0.35 for Rainy and Dry conditions, respectively
583 (Figure 6e, d)-6d, e). Again, this suggests that the UV-APS detects fungal spores as well as other types of
584 fluorescent particles. The R^2 values (~ 0.5) during Rainy periods indicate that the additional source of
585 particles detected by the UV-APS is likely to have a similar source, such as PBAP mechanically ejected
586 from soil and vegetative surfaces with rain-splash (Huffman et al., 2013). The magnitude of the over-
587 estimation is higher during Dry periods, which would be expected if as Rainy periods exhibited much
588 higher particle number fractions associated with polyol-containing spores.

589
590 The C11 cluster from WIBS data shows correlations with estimated fungal spores from arabitol
591 and mannitol that have slope much closer to 1.0 than correlations with UV-APS number (Figure 6e, f6g,
592 h, Table S3). For example, the slope of the C11 correlations with each polyol during Rainy periods is
593 approximately 0.87. This suggests only a 13% difference between the spore concentration estimates from
594 the two techniques during Rainy periods. The average number concentration of C11 during Rainy periods
595 is 1.6×10^4 (± 0.8) spores m^{-3} . In both cases the slopes with respect to C11 is greater than 1.0 during Dry
596 periods, suggesting that the cluster method may be missing some fraction of weakly fluorescent particles.
597 Huffman et al. (2012) similarly suggests that that particles that are weakly fluorescent may be below the
598 detection limit of the instrument, and Healy et al. (2014) suggested that both UV-APS and WIBS-4
599 instruments significantly under-count the ubiquitous *Cladosporium* spores that are most common during
600 dry weather and often peak in the afternoon when RH is low (De Groot, 1968; Oliveira et al., 2009).
601 Fundamentally, however, the results from the UV-APS, and even more so the numbers reported by the
602 clustering analysis by Crawford et al. (2015), reveal broadly similar trends with the numbers estimated
603 from polyol-to-spore values reported by Bauer et al. (2008a).

604
605 The fungal culture samples show similar division during Rainy and Dry periods as arabitol and
606 mannitol concentrations (Figure 6c), with an increase of approx. 1.6 during Rainy periods. The trend of a
607 positive slope with respect to the UV-LIF measurements is also similar between the tracer and culturing
608 methods. In general, however, the R^2 value correlating CFU to fungal spore number calculated from UV-
609 LIF number is lower than between tracers and UV-LIF numbers (Tables 2, S4). This is not unexpected for
610 several reasons. First, the short sampling time of the culture samples (20 min) leads to poor counting
611 statistics and high number concentration variability, whereas each data point from the high volume air
612 samples represents a period of 4 – 48 hours. Second, culture samplers, by their nature, only account for
613 culturable fungal spores. It has been estimated that as low as 17% of aerosolized fungal spores are
614 culturable, and so it is expected that the CFU concentration observed is significantly less than the total
615 airborne concentration of spores (Bridge and Spooner, 2001; Després et al., 2012). Nonetheless, the
616 culturing analysis here supports the tracer and UV-LIF analyses and the most important trends are
617 consistent between all analysis methods. The concentration of fungal spores is higher during the Rainy
618 periods, and there is a positive correlation between both tracer and CFU concentration and UV-LIF
619 number.

620
621 In pristine environment, such as the Amazon, supermicron particle mass has been found to consist
622 of up to 85% biological material (Pöschl et al., 2010). Total particulate matter mass was calculated here
623 from the UV-APS number concentrations (m^{-3}) and converted to mass for particles of aerodynamic
624 diameter 0.5 – 15 μm . In only this case a density of 1.5 $g\ cm^{-3}$ was utilized to calculate a first
625 approximation of total particle mass to which all other mass measurements were compared. An average
626 TSP mass density of 1.5 $g\ cm^{-3}$ was utilized, because organic aerosol is typically estimated with density <
627 1.0 $g\ cm^{-3}$, biological particles are often assumed to have ca. 1.0 $g\ cm^{-3}$ density, and mineral dust
628 particles have densities of up to ca. 3.5 $g\ cm^{-3}$ (Dexter, 2004; Tegen and Fung, 1994). Fungal spore mass
629 was estimated here using the fungal spore concentrations calculated from arabitol and mannitol mass (Fig.
630 6) and then using an estimated 33 pg reported by Bauer et al. (2008b) as an average mass per spore.
631 Dividing the resultant fungal spore mass by total particulate mass provides a relative mass fraction for
632 each high volume sample period. These calculations suggest that fungal spores represent approximately
633 23% \pm 9 (using arabitol) or 21% \pm 8 (using mannitol) of total particulate mass during Rainy periods
634 (Table 3, Figure 7). This represents a nearly 6 fold increase in percentage compared to Dry periods (4.8%
635 \pm 1.4 and 3.7% \pm 1.1, respectively). A similar increase during Rainy periods was also seen in the mass
636 fraction of fungal cluster Cl1, which represented 17% \pm 10 of the particle mass during Rainy and 2% \pm 1
637 during Dry periods (Table S4).

638 639 **3.5 Variations in endotoxin and glucan concentrations**

640 Endotoxins are components **uniquely** of gram-negative bacteria (Andreae and Crutzen, 1997).
641 Here, we show correlations between total endotoxin mass and WBS Cl_{Bact}, which were assigned by
642 Crawford et al. (2015) to be bacteria due to the small particle size (< 1 μm) and high correlation with rain.
643 These assignment of particle type to this set of clusters is quite uncertain, however, and should be treated
644 loosely. The correlation between endotoxin mass and UV-APS and the WBS clusters was very poor, in
645 most cases $R^2 < 0.1$ (Table 2, Figure 8), suggesting no apparent relationship. Analysis of bacteria by both
646 UV-LIF techniques is hampered by the fact that bacteria can be < 1 μm in size and because both
647 instruments detect particles with decreased efficiency at sizes below 0.8 μm . So weak correlations may
648 not have been apparent due to reduced overlap in particle size. Despite the lack of apparent correlation
649 between the techniques, the relatively variable endotoxin concentrations were elevated during Rainy
650 periods, consistent with Jones and Harrison (2004), who showed that bacteria concentration were elevated
651 after rainy periods.

652 Glucans, such as (1 \rightarrow 3)- β -D-glucan, are components of the cell walls of pollen, fungal spores,
653 plant detritus, and bacteria (Chow et al., 2015b; Lee et al., 2006; Stone and Clarke, 1992). In contrast to
654 the observed difference in endotoxin concentration during the different wetness periods, however, (1 \rightarrow 3)-

655 β -D-glucan showed no correlations with UV-LIF concentrations (Table 2) and no differentiation during
656 the different wetness periods.

657

658 4. Conclusions

659 Increased concentrations of fluorescent aerosol particles and ice nuclei attributed to having
660 biological origin were observed during and immediately after rain events throughout the BEACHON-
661 RoMBAS study in 2011 (Huffman et al., 2013; Prenni et al., 2013; Schumacher et al., 2013). Here we
662 expand upon the previous reports by utilizing measurements from two commercially available UV-LIF
663 instruments, of several molecular tracers extracted from high volume filter samples, and from a culture-
664 based sampler in order to compare three very different methods of atmospheric fungal spore analysis.
665 This study represents the first reported correlation of UV-LIF and molecular tracer measurements and
666 provided an opportunity to understand how an important class of PBAP might be influenced by periods of
667 rainy and dry weather. We found clear patterns in the fungal molecular tracers, arabitol and mannitol,
668 associated with Rainy conditions that are consistent with previous findings (Bauer et al., 2008a; Elbert et
669 al., 2007; Feofilova, 2001). Fungal polyols increased 3-fold over Dry conditions during Rainy weather
670 samples, with arabitol concentration of $35.2 \pm 10.5 \text{ ng m}^{-3}$ and mannitol concentration of $44.9 \pm 13.8 \text{ ng}$
671 m^{-3} . Additionally, the very high correlation of the fungal tracers with WIBS C11 ($R^2 > 0.8$ in many cases)
672 provides support for its assignment by Crawford et al. (2015) to fungal spores. Similarly, the UV-APS
673 correlates well with fungal tracers, however over-counts the number concentration estimated from the
674 tracers, confirming that the UV-APS is sensitive also to other types of particles beyond fungal spores, as
675 expected. The estimated spore count from the WIBS C11 concentration was within ~13% of the spore
676 count estimated by the tracer method, with concentrations ranging from $1.6 - 2.9 \times 10^4 \text{ spores m}^{-3}$. These
677 values are broadly consistent with concentrations modeled by, e.g. Spracklen and Heald (2014), Hoose et
678 al. (2010), and Hummel et al. (2015). These spore counts represent 17-23% of the total particle mass
679 during Rainy conditions and 2-4% during Dry conditions. Culture-based sampling also shows a similar
680 relationship between CFU and UV-LIF concentrations and an increase of ~1.6 between Dry and Rainy
681 conditions. Despite the fact that the tracer and UV-LIF approaches to estimating atmospheric fungal spore
682 concentration are fundamentally different, they provide remarkably similar estimates and temporal trends.
683 With further improvements in instrumentation and analysis methods (e.g. advanced clustering algorithms
684 applied to UV-LIF data), the ability to reliably discriminate between PBAP types is improving. As we
685 have shown here, this technology represents a potential for monitoring approximate fungal spore mass
686 and for contributing improved information on fungal spore concentration to global and regional models
687 that to this point has been lacking (Spracklen and Heald, 2014).

688

689

690 5. Acknowledgements

691 The BEACHON-RoMBAS campaign was partially supported by an ETBC (Emerging Topics in
692 Biogeochemical Cycles) grant to the National Center for Atmospheric Research (NCAR), the University
693 of Colorado, Colorado State University, and Penn State University (NSF ATM-0919189). The authors
694 wish to thank Jose Jimenez, Douglas Day (Univ. Colorado-Boulder); Anthony Prenni, Paul DeMott,
695 Sonia Kreidenweis, and Jessica Prenni (Colorado St. Univ.); Alex Guenther, and Jim Smith (NCAR) for
696 BEACHON-RoMBAS project organization and logistical support and the USFS, NCAR, and Richard
697 Oakes for access to the Manitou Experimental Forest Observatory field site. Measurements of
698 temperature, relative humidity, wind speed, and wind direction were provided by Andrew Turnipseed
699 (NCAR) and leaf wetness and disdrometer data were provided by Dave Gochis (NCAR). Marie I.
700 Gosselin thanks the Max Planck Society for financial support. J. Alex Huffman thanks the University of
701 Denver for intramural funding for faculty support. The Mainz team acknowledges the Mainz Bioaerosol
702 Laboratory (MBAL) and financial support from the Max Planck Society (MPG), the Max Planck
703 Graduate Center with the Johannes Gutenberg University Mainz (MPGC), the Geocycles Cluster Mainz
704 (LEC Rheinland-Pfalz), and the German Research Foundation (DFG PO1013/5-1 and FR3641/1-2, FOR
705 1525 INUIT). The Manchester team acknowledges funding from the UK NERC (UK-BEACHON, Grant

706 # NE/H019049/1) to participate in the BEACHON experiment, and development support of the WIBS
707 instruments. Manchester would also like to thank Prof. Paul Kaye, the developer of the WIBS instruments
708 and his team at the University of Hertfordshire, for their technical support. The authors thank Cristina
709 Ruzene, Isabell Müller-Germann, Petya Yordanova, Tobias Könnemann (Max Planck Inst. For Chem.),
710 and Nicole Savage (Univ. Denver) for technical assistance.
711
712

713 **6. References**

- 714
715 Allitt, U.: Airborne fungal spores and the thunderstorm of 24 June 1994, *Aerobiologia*, 16, 397-406,
716 2000.
- 717 Andreae, M. O. and Crutzen, P. J.: Atmospheric Aerosols: Biogeochemical Sources and Role in
718 Atmospheric Chemistry, *Science*, 276, 1052-1058, 10.1126/science.276.5315.1052, 1997.
- 719 Axelsson, B.-O., Saraf, A., and Larsson, L.: Determination of ergosterol in organic dust by gas
720 chromatography-mass spectrometry, *Journal of Chromatography B: Biomedical Sciences and*
721 *Applications*, 666, 77-84, [http://dx.doi.org/10.1016/0378-4347\(94\)00553-H](http://dx.doi.org/10.1016/0378-4347(94)00553-H), 1995.
- 722 Barbaro, E., Kirchgeorg, T., Zangrando, R., Vecchiato, M., Piazza, R., Barbante, C., and Gambaro, A.:
723 Sugars in Antarctic aerosol, *Atmos Environ*, 118, 135-144,
724 <http://dx.doi.org/10.1016/j.atmosenv.2015.07.047>, 2015.
- 725 Bauer, H., Claeys, M., Vermeylen, R., Schueller, E., Weinke, G., Berger, A., and Puxbaum, H.: Arabitol
726 and mannitol as tracers for the quantification of airborne fungal spores, *Atmos Environ*, 42, 588-593,
727 10.1016/j.atmosenv.2007.10.013, 2008a.
- 728 Bauer, H., Schueller, E., Weinke, G., Berger, A., Hitzemberger, R., Marr, I. L., and Puxbaum, H.:
729 Significant contributions of fungal spores to the organic carbon and to the aerosol mass balance of the
730 urban atmospheric aerosol, *Atmos Environ*, 42, 5542-5549, 10.1016/j.atmosenv.2008.03.019, 2008b.
- 731 Bigg, E. K., Soubeyrand, S., and Morris, C. E.: Persistent after-effects of heavy rain on concentrations of
732 ice nuclei and rainfall suggest a biological cause, *Atmos Chem Phys*, 15, 2313-2326, 2015.
- 733 Bridge, P. and Spooner, B.: Soil fungi: diversity and detection, *Plant and soil*, 232, 147-154, 2001.
- 734 Buller, A.: Spore deposits—the number of spores, *Researches on fungi*, 1, 79-88, 1909.
- 735 Burger, H.: Official Publication of American Academy of Allergy and Immunology Bioaerosols:
736 Prevalence and health effects in the indoor environment, *Journal of Allergy and Clinical Immunology*, 86,
737 687-701, [http://dx.doi.org/10.1016/S0091-6749\(05\)80170-8](http://dx.doi.org/10.1016/S0091-6749(05)80170-8), 1990.
- 738 Burshtein, N., Lang-Yona, N., and Rudich, Y.: Ergosterol, arabitol and mannitol as tracers for biogenic
739 aerosols in the eastern Mediterranean, *Atmos Chem Phys*, 11, 829-839, 10.5194/acp-11-829-2011, 2011.
- 740 Caseiro, A., Marr, I. L., Claeys, M., Kasper-Giebl, A., Puxbaum, H., and Pio, C. A.: Determination of
741 saccharides in atmospheric aerosol using anion-exchange high-performance liquid chromatography and
742 pulsed-amperometric detection, *Journal of Chromatography A*, 1171, 37-45,
743 <http://dx.doi.org/10.1016/j.chroma.2007.09.038>, 2007.
- 744 Cheng, J. Y. W., Hui, E. L. C., and Lau, A. P. S.: Bioactive and total endotoxins in atmospheric aerosols
745 in the Pearl River Delta region, China, *Atmos Environ*, 47, 3-11,
746 <http://dx.doi.org/10.1016/j.atmosenv.2011.11.055>, 2012.
- 747 Chow, J. C., Lowenthal, D. H., Chen, L.-W. A., Wang, X., and Watson, J. G.: Mass reconstruction
748 methods for PM_{2.5}: a review, *Air Quality, Atmosphere & Health*, 8, 243-263, 2015a.
- 749 Chow, J. C., Yang, X., Wang, X., Kohl, S. D., Hurbain, P. R., Chen, L. A., and Watson, J. G.:
750 Characterization of Ambient PM₁₀ Bioaerosols in a California Agricultural Town, *Aerosol Air Qual Res*,
751 15, 1433-1447, 2015b.

- 752 Crawford, I., Robinson, N. H., Flynn, M. J., Foot, V. E., Gallagher, M. W., Huffman, J. A., Stanley, W.
753 R., and Kaye, P. H.: Characterisation of bioaerosol emissions from a Colorado pine forest: results from
754 the BEACHON-RoMBAS experiment, *Atmos Chem Phys*, 14, 8559-8578, 10.5194/acp-14-8559-2014,
755 2014.
- 756 Crawford, I., Ruske, S., Topping, D., and Gallagher, M.: Evaluation of hierarchical agglomerative cluster
757 analysis methods for discrimination of primary biological aerosol, *Atmos Meas Tech*, 8, 4979-4991,
758 2015.
- 759 Dales, R. E., Cakmak, S., Judek, S., Dann, T., Coates, F., Brook, J. R., and Burnett, R. T.: The role of
760 fungal spores in thunderstorm asthma, *Chest*, 123, 745-750, 2003.
- 761 De Groot, R.: Diurnal cycles of air-borne spores produced by forest fungi, *Phytopathology*, 58, 1223-
762 1229, 1968.
- 763 Deguillaume, L., Leriche, M., Amato, P., Ariya, P. A., Delort, A. M., Pöschl, U., Chaumerliac, N., Bauer,
764 H., Flossmann, A. I., and Morris, C. E.: Microbiology and atmospheric processes: chemical interactions
765 of primary biological aerosols, *Biogeosciences*, 5, 1073-1084, 10.5194/bg-5-1073-2008, 2008.
- 766 Després, V. R., Huffman, J. A., Burrows, S. M., Hoose, C., Safatov, A. S., Buryak, G., Fröhlich-
767 Nowoisky, J., Elbert, W., Andreae, M. O., Poschl, U., and Jaenicke, R.: Primary biological aerosol
768 particles in the atmosphere: a review, *Tellus B*, 64, 58, Artn 15598 10.3402/Tellusb.V64i0.15598, 2012.
- 769 Dexter, A.: Soil physical quality: Part I. Theory, effects of soil texture, density, and organic matter, and
770 effects on root growth, *Geoderma*, 120, 201-214, 2004.
- 771 Di Filippo, P., Pomata, D., Riccardi, C., Buiarelli, F., and Perrino, C.: Fungal contribution to size-
772 segregated aerosol measured through biomarkers, *Atmos Environ*, 64, 132-140, 2013.
- 773 Douwes, J., Thorne, P., Pearce, N., and Heederik, D.: Bioaerosol health effects and exposure assessment:
774 progress and prospects, *Annals of Occupational Hygiene*, 47, 187-200, 2003.
- 775 Elbert, W., Taylor, P. E., Andreae, M. O., and Poschl, U.: Contribution of fungi to primary biogenic
776 aerosols in the atmosphere: wet and dry discharged spores, carbohydrates, and inorganic ions, *Atmos
777 Chem Phys*, 7, 4569-4588, 2007.
- 778 Faulwetter, R.: Wind-blown rain, a factor in disease dissemination, *J. agric. Res*, 10, 639-648, 1917.
- 779 Feofilova, E. P.: The Kingdom Fungi: Heterogeneity of Physiological and Biochemical Properties and
780 Relationships with Plants, Animals, and Prokaryotes (Review), *Applied Biochemistry and Microbiology*,
781 37, 124-137, 10.1023/a:1002863311534, 2001.
- 782 Foot, V. E., Kaye, P. H., Stanley, W. R., Barrington, S. J., Gallagher, M., and Gabey, A.: Low-cost real-
783 time multiparameter bio-aerosol sensors, 2008, 71160I-71160I-71112.
- 784 Frankland, A. and Gregory, P.: Allergenic and agricultural implications of airborne ascospore
785 concentrations from a fungus, *Didymella exitialis*, 1973. 1973.
- 786 Fröhlich-Nowoisky, J., Burrows, S., Xie, Z., Engling, G., Solomon, P., Fraser, M., Mayol-Bracero, O.,
787 Artaxo, P., Begerow, D., and Conrad, R.: Biogeography in the air: fungal diversity over land and oceans,
788 *Biogeosciences*, 9, 1125-1136, 2012.
- 789 Fröhlich-Nowoisky, J., Kampf, C. J., Weber, B., Huffman, J. A., Pöhlker, C., Andreae, M. O., Lang-
790 Yona, N., Burrows, S. M., Gunthe, S. S., Elbert, W., Su, H., Hoor, P., Thines, E., Hoffmann, T., Després,

791 V. R., Pöschl, U.: Bioaerosols in the Earth System: Climate, Health, and Ecosystem Interactions,
792 Atmospheric Research, 182, 346-376, 10.1016/j.atmosres.2016.07.018, 2016.

793 Fröhlich-Nowoisky, J., Pickersgill, D. A., Després, V. R., and Pöschl, U.: High diversity of fungi in air
794 particulate matter, Proceedings of the National Academy of Sciences, 106, 12814-12819, 2009.

795 Gabey, A., Gallagher, M., Whitehead, J., Dorsey, J., Kaye, P. H., and Stanley, W.: Measurements and
796 comparison of primary biological aerosol above and below a tropical forest canopy using a dual channel
797 fluorescence spectrometer, Atmos Chem Phys, 10, 4453-4466, 2010.

798 Gilardoni, S., Vignati, E., Marmer, E., Cavalli, F., Belis, C., Gianelle, V., Loureiro, A., and Artaxo, P.:
799 Sources of carbonaceous aerosol in the Amazon basin, Atmos Chem Phys, 11, 2747-2764, 2011.

800 Gonçalves, F. L. T., Bauer, H., Cardoso, M. R. A., Pukinskas, S., Matos, D., Melhem, M., and Puxbaum,
801 H.: Indoor and outdoor atmospheric fungal spores in the São Paulo metropolitan area (Brazil): species and
802 numeric concentrations, International journal of biometeorology, 54, 347-355, 2010.

803 Graham, B., Guyon, P., Taylor, P. E., Artaxo, P., Maenhaut, W., Glovsky, M. M., Flagan, R. C., and
804 Andreae, M. O.: Organic compounds present in the natural Amazonian aerosol: Characterization by gas
805 chromatography-mass spectrometry, J Geophys Res-Atmos, 108, 4766-4766, 10.1029/2003jd003990,
806 2003.

807 Gregory, P. H. and Sreeramulu, T.: Air spora of an estuary, T Brit Mycol Soc, 41, 145-156,
808 [http://dx.doi.org/10.1016/S0007-1536\(58\)80025-X](http://dx.doi.org/10.1016/S0007-1536(58)80025-X), 1958.

809 Haga, D., Iannone, R., Wheeler, M., Mason, R., Polishchuk, E., Fetch, T., Kamp, B., McKendry, I., and
810 Bertram, A.: Ice nucleation properties of rust and bunt fungal spores and their transport to high altitudes,
811 where they can cause heterogeneous freezing, Journal of Geophysical Research: Atmospheres, 118, 7260-
812 7272, 2013.

813 Hairston, P. P., Ho, J., and Quant, F. R.: Design of an instrument for real-time detection of bioaerosols
814 using simultaneous measurement of particle aerodynamic size and intrinsic fluorescence, Journal of
815 Aerosol Science, 28, 471-482, 1997.

816 Heald, C. L. and Spracklen, D. V.: Atmospheric budget of primary biological aerosol particles from
817 fungal spores, Geophysical Research Letters, 36, L09806/09801-L09806/09805, 2009.

818 Healy, D., Huffman, J., O'Connor, D., Pöhlker, C., Pöschl, U., and Sodeau, J.: Ambient measurements of
819 biological aerosol particles near Killarney, Ireland: a comparison between real-time fluorescence and
820 microscopy techniques, Atmos Chem Phys, 14, 8055-8069, 2014.

821 Hernandez, M., Perring, A. E., McCabe, K., Kok, G., Granger, G., and Baumgardner, D.: Chamber
822 catalogues of optical and fluorescent signatures distinguish bioaerosol classes, Atmos Meas Tech, 9,
823 3283-3292, 2016.

824 Hill, S. C., Mayo, M. W., and Chang, R. K.: Fluorescence of bacteria, pollens, and naturally occurring
825 airborne particles: excitation/emission spectra, DTIC Document, 2009.

826 Hill, S. C., Pan, Y.-L., Williamson, C., Santarpia, J. L., and Hill, H. H.: Fluorescence of bioaerosols:
827 mathematical model including primary fluorescing and absorbing molecules in bacteria, Optics Express,
828 21, 22285-22313, 10.1364/oe.21.022285, 2013.

829 Hill, S. C., Williamson, C. C., Doughty, D. C., Pan, Y.-L., Santarpia, J. L., and Hill, H. H.: Size-
830 dependent fluorescence of bioaerosols: Mathematical model using fluorescing and absorbing molecules in

831 bacteria, *Journal of Quantitative Spectroscopy and Radiative Transfer*, 157, 54-70,
832 <http://dx.doi.org/10.1016/j.jqsrt.2015.01.011>, 2015.

833 Hirst, J. and Stedman, O.: Dry liberation of fungus spores by raindrops, *Microbiology*, 33, 335-344, 1963.

834 Hoose, C., Kristjánsson, J. E., Chen, J.-P., and Hazra, A.: A Classical-Theory-Based Parameterization of
835 Heterogeneous Ice Nucleation by Mineral Dust, Soot, and Biological Particles in a Global Climate Model,
836 *Journal of the Atmospheric Sciences*, 67, 2483-2503, doi:10.1175/2010JAS3425.1, 2010.

837 Huffman, J. A., Prenni, A. J., DeMott, P. J., Pöhlker, C., Mason, R. H., Robinson, N. H., Fröhlich-
838 Nowoisky, J., Tobo, Y., Després, V. R., Garcia, E., Gochis, D. J., Harris, E., Müller-Germann, I., Ruzene,
839 C., Schmer, B., Sinha, B., Day, D. A., Andreae, M. O., Jimenez, J. L., Gallagher, M., Kreidenweis, S. M.,
840 Bertram, A. K., and Pöschl, U.: High concentrations of biological aerosol particles and ice nuclei during
841 and after rain, *Atmos. Chem. Phys.*, 13, 6151-6164, 10.5194/acp-13-6151-2013, 2013.

842 Huffman, J. A. and Santarpia, J.: Online techniques for quantification and characterization of biological
843 aerosol. In: *Microbiology of aerosols*, Delort, A.-M. and Amato, P. (Eds.), Wiley, Hoboken, NJ, 2016.

844 Huffman, J. A., Sinha, B., Garland, R. M., Snee-Pollmann, A., Gunthe, S. S., Artaxo, P., Martin, S. T.,
845 Andreae, M. O., and Pöschl, U.: Size distributions and temporal variations of biological aerosol particles
846 in the Amazon rainforest characterized by microscopy and real-time UV-APS fluorescence techniques
847 during AMAZE-08, *Atmos. Chem. Phys.*, 12, 11997-12019, 10.5194/acp-12-11997-2012, 2012.

848 Hummel, M., Hoose, C., Gallagher, M., Healy, D. A., Huffman, J. A., O'Connor, D., Poeschl, U.,
849 Poehlker, C., Robinson, N. H., Schnaiter, M., Sodeau, J. R., Stengel, M., Toprak, E., and Vogel, H.:
850 Regional-scale simulations of fungal spore aerosols using an emission parameterization adapted to local
851 measurements of fluorescent biological aerosol particles, *Atmos Chem Phys*, 15, 6127-6146, 2015.

852 Ingold, C. T.: Fungal spores. Their liberation and dispersal, *Fungal spores. Their liberation and dispersal.*,
853 1971. 1971.

854 Jones, A. M. and Harrison, R. M.: The effects of meteorological factors on atmospheric bioaerosol
855 concentrations—a review, *Science of the Total Environment*, 326, 151-180,
856 <http://dx.doi.org/10.1016/j.scitotenv.2003.11.021>, 2004.

857 Kaye, P., Stanley, W., Hirst, E., Foot, E., Baxter, K., and Barrington, S.: Single particle multichannel bio-
858 aerosol fluorescence sensor, *Optics Express*, 13, 3583-3593, 2005.

859 Lau, A. P. S., Lee, A. K. Y., Chan, C. K., and Fang, M.: Ergosterol as a biomarker for the quantification
860 of the fungal biomass in atmospheric aerosols, *Atmos Environ*, 40, 249-259, 2006.

861 Laumbach, R. J. and Kipen, H. M.: Bioaerosols and sick building syndrome: particles, inflammation, and
862 allergy, *Current opinion in allergy and clinical immunology*, 5, 135-139, 2005.

863 Lee, T., Grinshpun, S. A., Kim, K. Y., Iossifova, Y., Adhikari, A., and Reponen, T.: Relationship between
864 indoor and outdoor airborne fungal spores, pollen, and (1→3)-β-D-glucan in homes without visible mold
865 growth, *Aerobiologia*, 22, 227-235, 2006.

866 Lee, T., Sullivan, A. P., Mack, L., Jimenez, J. L., Kreidenweis, S. M., Onasch, T. B., Worsnop, D. R.,
867 Malm, W., Wold, C. E., Hao, W. M., and Collett, J. L., Jr.: Chemical Smoke Marker Emissions During
868 Flaming and Smoldering Phases of Laboratory Open Burning of Wildland Fuels, *Aerosol Science and*
869 *Technology*, 44, I-V, 2010.

- 870 Lewis, D. H. and Smith, D. C.: Sugar alcohols (polyols) in fungi and green plants, *New Phytol*, 66, 185-
871 204, 1967.
- 872 Liang, L., Engling, G., He, K., Du, Z., Cheng, Y., and Duan, F.: Evaluation of fungal spore characteristics
873 in Beijing, China, based on molecular tracer measurements, *Environmental Research Letters*, 8, 014005,
874 2013.
- 875 Lin, W.-H. and Li, C.-S.: Associations of fungal aerosols, air pollutants, and meteorological factors,
876 *Aerosol Science & Technology*, 32, 359-368, 2000.
- 877 Linneberg, A.: The increase in allergy and extended challenges, *Allergy*, 66, 1-3, 2011.
- 878 Madden, L.: Effects of rain on splash dispersal of fungal pathogens, *Canadian Journal of Plant Pathology*,
879 19, 225-230, 1997.
- 880 Madelin, T.: Fungal aerosols: a review, *Journal of Aerosol Science*, 25, 1405-1412, 1994.
- 881 Miller, J. D. and Young, J. C.: The use of ergosterol to measure exposure to fungal propagules in indoor
882 air, *American Industrial Hygiene Association Journal*, 58, 39-43, 1997.
- 883 Morris, C., Sands, D., Glaux, C., Samsatly, J., Asaad, S., Moukahel, A., Goncalves, F. L. T., and Bigg, E.:
884 Urediospores of rust fungi are ice nucleation active at >-10 C and harbor ice nucleation active bacteria,
885 *Atmos Chem Phys*, 13, 4223-4233, 2013.
- 886 Oliveira, M., Ribeiro, H., Delgado, J., and Abreu, I.: The effects of meteorological factors on airborne
887 fungal spore concentration in two areas differing in urbanisation level, *International journal of*
888 *biometeorology*, 53, 61-73, 2009.
- 889 Ortega, J., Turnipseed, A., Guenther, A. B., Karl, T. G., Day, D. A., Gochis, D., Huffman, J. A., Prenni,
890 A. J., Levin, E. J. T., Kreidenweis, S. M., DeMott, P. J., Tobo, Y., Patton, E. G., Hodzic, A., Cui, Y. Y.,
891 Harley, P. C., Hornbrook, R. S., Apel, E. C., Monson, R. K., Eller, A. S. D., Greenberg, J. P., Barth, M.
892 C., Campuzano-Jost, P., Palm, B. B., Jimenez, J. L., Aiken, A. C., Dubey, M. K., Geron, C., Offenberg,
893 J., Ryan, M. G., Fornwalt, P. J., Pryor, S. C., Keutsch, F. N., DiGangi, J. P., Chan, A. W. H., Goldstein,
894 A. H., Wolfe, G. M., Kim, S., Kaser, L., Schnitzhofer, R., Hansel, A., Cantrell, C. A., Mauldin, R. L., and
895 Smith, J. N.: Overview of the Manitou Experimental Forest Observatory: site description and selected
896 science results from 2008 to 2013, *Atmos Chem Phys*, 14, 6345-6367, 10.5194/acp-14-6345-2014, 2014.
- 897 Perring, A., Schwarz, J., Baumgardner, D., Hernandez, M., Spracklen, D., Heald, C., Gao, R., Kok, G.,
898 McMeeking, G., and McQuaid, J.: Airborne observations of regional variation in fluorescent aerosol
899 across the United States, *Journal of Geophysical Research: Atmospheres*, 120, 1153-1170, 2015.
- 900 Pöhlker, C., Huffman, J. A., Forster, J. D., and Pöschl, U.: Autofluorescence of atmospheric bioaerosols:
901 spectral fingerprints and taxonomic trends of pollen, *Atmos Meas Tech*, 6, 3369-3392, 10.5194/amt-6-
902 3369-2013, 2013.
- 903 Pöhlker, C., Huffman, J. A., and Pöschl, U.: Autofluorescence of atmospheric bioaerosols-fluorescent
904 biomolecules and potential interferences, *Atmos Meas Tech*, 5, 37-71, 2012a.
- 905 Pöhlker, C., Wiedemann, K. T., Sinha, B., Shiraiwa, M., Gunthe, S. S., Smith, M., Su, H., Artaxo, P.,
906 Chen, Q., and Cheng, Y.: Biogenic potassium salt particles as seeds for secondary organic aerosol in the
907 Amazon, *Science*, 337, 1075-1078, 2012b.

908 Pöschl, U., Martin, S., Sinha, B., Chen, Q., Gunthe, S., Huffman, J., Borrmann, S., Farmer, D., Garland,
909 R., and Helas, G.: Rainforest aerosols as biogenic nuclei of clouds and precipitation in the Amazon,
910 *Science*, 329, 1513-1516, 2010.

911 Pöschl, U. and Shiraiwa, M.: Multiphase chemistry at the atmosphere–biosphere interface influencing
912 climate and public health in the Anthropocene, *Chemical reviews*, 115, 4440-4475, 2015.

913 Prenni, A. J., Tobo, Y., Garcia, E., DeMott, P. J., Huffman, J. A., McCluskey, C. S., Kreidenweis, S. M.,
914 Prenni, J. E., Pöhlker, C., and Pöschl, U.: The impact of rain on ice nuclei populations at a forested site in
915 Colorado, *Geophysical Research Letters*, 40, 227-231, 10.1029/2012gl053953, 2013.

916 Pyrri, I. and Kapsanaki-Gotsi, E.: A comparative study on the airborne fungi in Athens, Greece, by viable
917 and non-viable sampling methods, *Aerobiologia*, 23, 3-15, 2007.

918 Rasband, W. and ImageJ, U.: Bethesda, Md, USA. ImageJ, 1997.

919 Rathnayake, C. M., Metwali, N., Baker, Z., Jayarathne, T., Kostle, P. A., Thorne, P. S., O'Shaughnessy, P.
920 T., and Stone, E. A.: Urban enhancement of PM10 bioaerosol tracers relative to background locations in
921 the Midwestern United States, *Journal of Geophysical Research: Atmospheres*, 121, 5071-5089, 2016a.

922 Rathnayake, C. M., Metwali, N., Jayarathne, T., Kettler, J., Huang, Y., Thorne, P. S., O'Shaughnessy, P.
923 T., and Stone, E. A.: Influence of Rain on the Abundance and Size Distribution of Bioaerosols, *Atmos.*
924 *Chem. Phys. Discuss.*, 2016, 1-29, 10.5194/acp-2016-622, 2016b.

925 Robinson, N. H., Allan, J. D., Huffman, J. A., Kaye, P. H., Foot, V. E., and Gallagher, M.: Cluster
926 analysis of WBS single-particle bioaerosol data, *Atmos Meas Tech*, 6, 337-347, 10.5194/amt-6-337-
927 2013, 2013.

928 Ruske, S., Topping, D. O., Foot, V. E., Kaye, P. H., Stanley, W. R., Crawford, I., Morse, A. P., and
929 Gallagher, M. W.: Evaluation of Machine Learning Algorithms for Classification of Primary Biological
930 Aerosol using a new UV-LIF spectrometer, 2016. 2016.

931 Saari, S., Niemi, J., Rönkkö, T., Kuuluvainen, H., Järvinen, A., Pirjola, L., Aurela, M., Hillamo, R., and
932 Keskinen, J.: Seasonal and diurnal variations of fluorescent bioaerosol concentration and size distribution
933 in the urban environment, *Aerosol and Air Quality Research*, 15, 572-581, 2015.

934 Saari, S., Putkiranta, M., and Keskinen, J.: Fluorescence spectroscopy of atmospherically relevant
935 bacterial and fungal spores and potential interferences, *Atmos Environ*, 71, 202-209, 2013.

936 Schauer, J. J., Rogge, W. F., Hildemann, L. M., Mazurek, M. A., Cass, G. R., and Simoneit, B. R. T.:
937 Source apportionment of airborne particulate matter using organic compounds as tracers, *Atmos Environ*,
938 30, 3837-3855, [http://dx.doi.org/10.1016/1352-2310\(96\)00085-4](http://dx.doi.org/10.1016/1352-2310(96)00085-4), 1996.

939 Schumacher, C. J., Pöhlker, C., Aalto, P., Hiltunen, V., Petäjä, T., Kulmala, M., Pöschl, U., and Huffman,
940 J. A.: Seasonal cycles of fluorescent biological aerosol particles in boreal and semi-arid forests of Finland
941 and Colorado, *Atmos. Chem. Phys.*, 13, 11987-12001, 10.5194/acp-13-11987-2013, 2013.

942 Sesartic, A. and Dallafior, T. N.: Global fungal spore emissions, review and synthesis of literature data,
943 *Biogeosciences*, 8, 1181-1192, 10.5194/bg-8-1181-2011, 2011.

944 Sesartic, A., Lohmann, U., and Storelvmo, T.: Modelling the impact of fungal spore ice nuclei on clouds
945 and precipitation, *Environmental Research Letters*, 8, 014029, 2013.

- 946 Simoneit, B. R. and Mazurek, M.: Organic tracers in ambient aerosols and rain, *Aerosol Science and*
947 *Technology*, 10, 267-291, 1989.
- 948 Simoneit, B. R. T., Kobayashi, M., Mochida, M., Kawamura, K., Lee, M., Lim, H.-J., Turpin, B. J., and
949 Komazaki, Y.: Composition and major sources of organic compounds of aerosol particulate matter
950 sampled during the ACE-Asia campaign, *Journal of Geophysical Research*, [Atmospheres], 109,
951 D19S10/11-D19S10/22, 2004.
- 952 Sodeau, J. and O'Connor, D.: Bioaerosol Monitoring of the Atmosphere for Occupational and
953 Environmental Purposes, *Comprehensive Analytical Chemistry*, 2016. 2016.
- 954 Spracklen, D. and Heald, C. L.: The contribution of fungal spores and bacteria to regional and global
955 aerosol number and ice nucleation immersion freezing rates, *Atmos Chem Phys*, 14, 9051-9059, 2014.
- 956 Stone, B. and Clarke, A.: Chemistry and biology of (1, 3)-D-glucans, Victoria, Australia.: La Trobe
957 University Press, 1992. 236-239, 1992.
- 958 Taylor, P. E. and Jonsson, H.: Thunderstorm asthma, *Current allergy and asthma reports*, 4, 409-413,
959 2004.
- 960 Tegen, I. and Fung, I.: Modeling of mineral dust in the atmosphere: Sources, transport, and optical
961 thickness, *Journal of Geophysical Research: Atmospheres*, 99, 22897-22914, 1994.
- 962 Tobo, Y., Prenni, A. J., DeMott, P. J., Huffman, J. A., McCluskey, C. S., Tian, G., Pöhlker, C., Pöschl,
963 U., and Kreidenweis, S. M.: Biological aerosol particles as a key determinant of ice nuclei populations in
964 a forest ecosystem, *Journal of Geophysical Research: Atmospheres*, 118, 10,100-110,110,
965 10.1002/jgrd.50801, 2013.
- 966 Toprak, E. and Schnaiter, M.: Fluorescent biological aerosol particles measured with the Waveband
967 Integrated Bioaerosol Sensor WIBS-4: laboratory tests combined with a one year field study, *Atmos.*
968 *Chem. Phys*, 13, 225-243, 2013.
- 969 Weete, J. D.: Sterols of the fungi: distribution and biosynthesis, *Phytochemistry*, 12, 1843-1864, 1973.
- 970 Womiloju, T. O., Miller, J. D., Mayer, P. M., and Brook, J. R.: Methods to determine the biological
971 composition of particulate matter collected from outdoor air, *Atmos Environ*, 37, 4335-4344, 2003.
- 972 Yang, Y., Chan, C.-y., Tao, J., Lin, M., Engling, G., Zhang, Z., Zhang, T., and Su, L.: Observation of
973 elevated fungal tracers due to biomass burning in the Sichuan Basin at Chengdu City, China, *Science of*
974 *the Total Environment*, 431, 68-77, 2012.
- 975 Yttri, K. E., Simpson, D., Noejaard, J. K., Kristensen, K., Genberg, J., Stenstrom, K., Swietlicki, E.,
976 Hillamo, R., Aurela, M., Bauer, H., Offenbergh, J. H., Jaoui, M., Dye, C., Eckhardt, S., Burkhardt, J. F.,
977 Stohl, A., and Glasius, M.: Source apportionment of the summer time carbonaceous aerosol at Nordic
978 rural background sites, *Atmos Chem Phys*, 11, 13339-13357, 2011a.
- 979 Yttri, K. E., Simpson, D., Stenstrom, K., Puxbaum, H., and Svendby, T.: Source apportionment of the
980 carbonaceous aerosol in Norway - quantitative estimates based on ¹⁴C, thermal-optical and organic tracer
981 analysis, *Atmos Chem Phys*, 11, 9375-9394, 2011b.
- 982 Yue, S., Ren, H., Fan, S., Sun, Y., Wang, Z., and Fu, P.: Springtime precipitation effects on the
983 abundance of fluorescent biological aerosol particles and HULIS in Beijing, *Scientific Reports*, 6, 2016.

- 984 Zhang, T., Engling, G., Chan, C.-Y., Zhang, Y.-N., Zhang, Z.-S., Lin, M., Sang, X.-F., Li, Y. D., and Li,
985 Y.-S.: Contribution of fungal spores to particulate matter in a tropical rainforest, *Environmental Research*
986 *Letters*, 5, No pp. given, 2010.
- 987 Zhang, Z., Engling, G., Zhang, L., Kawamura, K., Yang, Y., Tao, J., Zhang, R., Chan, C.-y., and Li, Y.:
988 Significant influence of fungi on coarse carbonaceous and potassium aerosols in a tropical rainforest,
989 *Environmental Research Letters*, 10, 1-9, 2015.
- 990 Zhu, C., Kawamura, K., and Kunwar, B.: Organic tracers of primary biological aerosol particles at
991 subtropical Okinawa Island in the western North Pacific Rim, *Journal of Geophysical Research:*
992 *Atmospheres*, 120, 5504-5523, 10.1002/2015jd023611, 2015.
- 993

994

995 **Tables and Figures:**

996

| | | | Mass Concentration | | | | | |
|--------------------|---|-------|-----------------------------------|-------|-----------------------------------|-------|---|-------|
| | | | Arabitol (ng m ⁻³) | | Mannitol (ng m ⁻³) | | (1→3)-β-D-glucan (pg m ⁻³) | |
| | | | Rainy | Dry | Rainy | Dry | Rainy | Dry |
| Mass Concentration | Mannitol (ng m ⁻³) | Rainy | <u>0.839</u> | | | | | |
| | | Dry | | 0.312 | | | | |
| | (1→3)-β-D-glucan (pg m ⁻³) | Rainy | 0.000 | | 0.003 | | | |
| | | Dry | | 0.000 | | 0.327 | | |
| | Endotoxins (EU m ⁻³) | Rainy | 0.116 | | 0.126 | | 0.427 | |
| | | Dry | | 0.012 | | 0.113 | | 0.103 |

997

998 **Table 1:** Square of correlation coefficients (R²) comparing total mass concentration of molecular tracers

999 to each other. EU: endotoxin units. Boxes colored by coefficient value (**Bold Underline** > 0.7; 0.7 > **Bold**

1000 > 0.4).

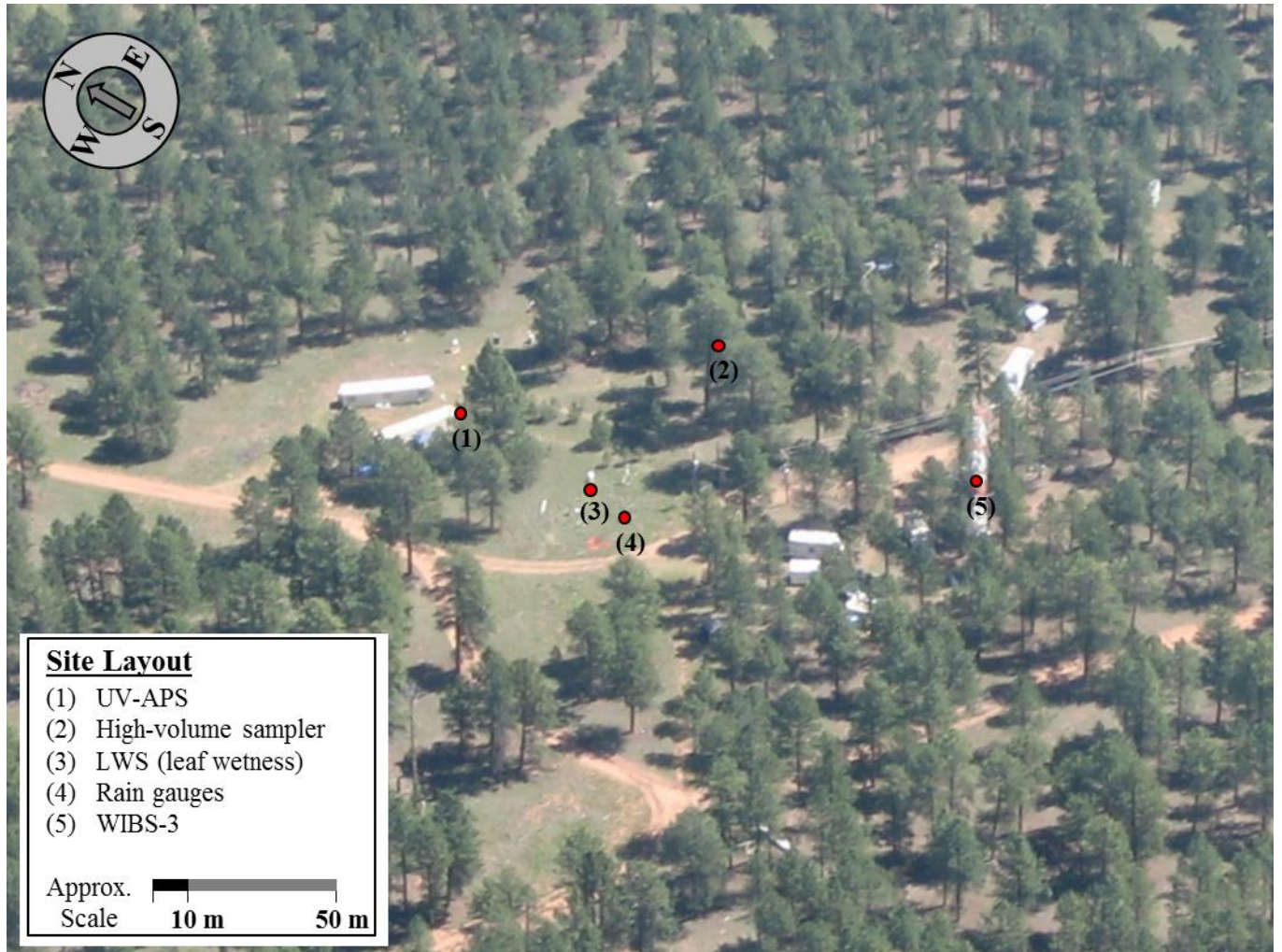
| | | | Mass Concentration | | | | | | | | Fungal Spore Number Conc. | | | | | | |
|-------------------------------------|-------|-----|--------------------------------|---------------------|--------------------------------|---------------------|--|-------|----------------------------------|-------|------------------------------------|--------------|------------------------------------|---------------------|---|--------------|---------------------|
| | | | Arabitol (ng m ⁻³) | | Mannitol (ng m ⁻³) | | (1→3)-β-D-glucan (pg m ⁻³) | | Endotoxins (EU m ⁻³) | | Arabitol (spores m ⁻³) | | Mannitol (spores m ⁻³) | | Colony Forming Units (CFU m ⁻³) | | |
| | | | Rainy | Dry | Rainy | Dry | Rainy | Dry | Rainy | Dry | Rainy | Dry | Rainy | Dry | Rainy | Dry | |
| UV-LIF Mass or Number Concentration | UVAPS | | <u>0.732</u> | 0.127 | <u>0.877</u> | 0.160 | 0.006 | 0.012 | 0.153 | 0.067 | 0.483 | 0.278 | 0.504 | 0.571 | 0.469 | 0.491 | |
| | WIBS | FL | | 0.554 | 0.250 | <u>0.810</u> | 0.255 | 0.128 | 0.010 | 0.068 | 0.066 | 0.159 | 0.200 | 0.088 | 0.314 | 0.330 | <u>0.737</u> |
| | | FL1 | | 0.602 | 0.445 | <u>0.819</u> | 0.412 | 0.042 | 0.001 | 0.090 | 0.012 | 0.667 | 0.339 | <u>0.863</u> | 0.621 | 0.470 | 0.546 |
| | | FL2 | | 0.617 | 0.248 | <u>0.843</u> | 0.342 | 0.092 | 0.001 | 0.039 | 0.094 | 0.485 | 0.302 | 0.442 | 0.340 | 0.560 | 0.543 |
| | | FL3 | | 0.561 | 0.222 | <u>0.818</u> | 0.251 | 0.124 | 0.008 | 0.071 | 0.065 | 0.178 | 0.181 | 0.104 | 0.306 | 0.367 | <u>0.736</u> |
| | | Cl1 | | <u>0.824</u> | <u>0.764</u> | <u>0.799</u> | 0.109 | 0.000 | 0.134 | 0.229 | 0.011 | 0.679 | 0.543 | <u>0.775</u> | 0.423 | 0.128 | 0.690 |
| | | Cl2 | | 0.005 | 0.002 | 0.004 | 0.006 | 0.002 | 0.047 | 0.006 | 0.017 | 0.052 | 0.056 | 0.001 | 0.075 | 0.081 | <u>0.930</u> |
| | | Cl3 | | 0.267 | 0.164 | 0.261 | 0.198 | 0.003 | 0.011 | 0.016 | 0.066 | 0.052 | 0.116 | 0.087 | 0.439 | 0.262 | 0.383 |
| | | Cl4 | | 0.048 | 0.046 | 0.172 | 0.118 | 0.115 | 0.011 | 0.179 | 0.145 | 0.062 | 0.089 | 0.001 | 0.065 | 0.120 | 0.000 |
| Cl _{Bact} | | | | | | | | 0.041 | 0.081 | | | | | | | | |

1001 **Table 2:** Square of correlation coefficients (R^2) comparing fluorescent particle measurements from UV-LIF instruments to measurements from
1002 molecular tracers. Columns marking tracer mass (top line) indicate correlations between time-averaged UV-LIF and tracer mass concentrations
1003 (left side), and columns marking fungal spore number indicate correlations between fungal spore number concentrations estimated from time-
1004 averaged UV-LIF and tracer or culture measurements (right side). FL1, FL2, FL3 represent individual channels from the WIBS. FL represents all
1005 particle exhibiting fluorescence in any channel. Cl1, Cl2, Cl3, Cl4 are clusters that estimate particle concentrations as a mixture of various
1006 channels (Crawford et al., 2015). Cl_{Bact} is a sum of the “bacteria” clusters Cl2-4. Boxes colored by coefficient value (**Bold Underline** > 0.7; **0.7 >**
1007 **Bold** > 0.4).

| | Mass Concentration | | | | | | |
|-------|--|-----------------------------------|-------------------------------------|---------------------------------------|----------------------------------|-------------------------------------|---|
| | Arabitol (ng m ⁻³) | Mannitol (ng m ⁻³) | Erythritol (ng m ⁻³) | Levoglucozan (ng m ⁻³) | Glucose (ng m ⁻³) | Endotoxins (EU m ⁻³) | (1→3)-β-D- glucan (pg m ⁻³) |
| Dry | 10.6 ± 2.5 n = 18 | 11.9 ± 3.2 n=18 | 0.840 ± 0.610 n=16 | 14.2 ± 10.7 n=15 | 38.7 ± 21.3 n=18 | 0.192 ± 0.0970 n=18 | 8.8 5 ± 7.68 n=18 |
| Rainy | 35.2 ± 10.5 n=11 | 44.9 ± 13.8 n=11 | 1.12 ± 0.38 n=3 | 12.4 ± 19.1 n=8 | 73.2 ± 50.5 n=11 | 1.43 ± 1.22 n=10 | 10.6 ± 8.2 n=11 |
| Other | 20.2 ± 8.9 n=6 | 22.7 ± 8.3 n=6 | 0.664 ± 0.515 n=6 | 9.21 ± 1.66 n=5 | 56.5 ± 39.2 n=6 | 0.311 ± 0.159 n=6 | 6.08 ± 6.08 n=6 |
| | Mass Contribution (%) | | | | | | |
| Dry | 0.18 % ± 0.05 n=18 | 0.202 % ± 0.073 n=18 | 0.014 % ± 0.011 n=16 | 0.21 % ±0.17 n=15 | 0.67 % ±0.49 n=18 | | 0.16 % ±0.16 n=18 |
| Rainy | 0.83 % ± 0.32 n=11 | 1.07 % ±0.44 n=11 | 0.032 % ±0.009 n=3 | 0.27 % ±0.41 n=8 | 1.60 % ±1.09 n=11 | | 0.25 % ±0.21 n=11 |
| Other | 0.25 % ± 0.28 n=6 | 0.37 % ± 0.29 n=6 | 0.013 % ±0.015 n=6 | 0.15 % ±0.11 n=5 | 0.83 % ±0.64 n=6 | | 0.12 % ±0.19 n=6 |
| | Fungal Spore Number Concentration (m ⁻³) | | | | | | |
| Dry | 8870 ± 2060 n=18 | 6890 ± 1870 n=18 | | | | | |

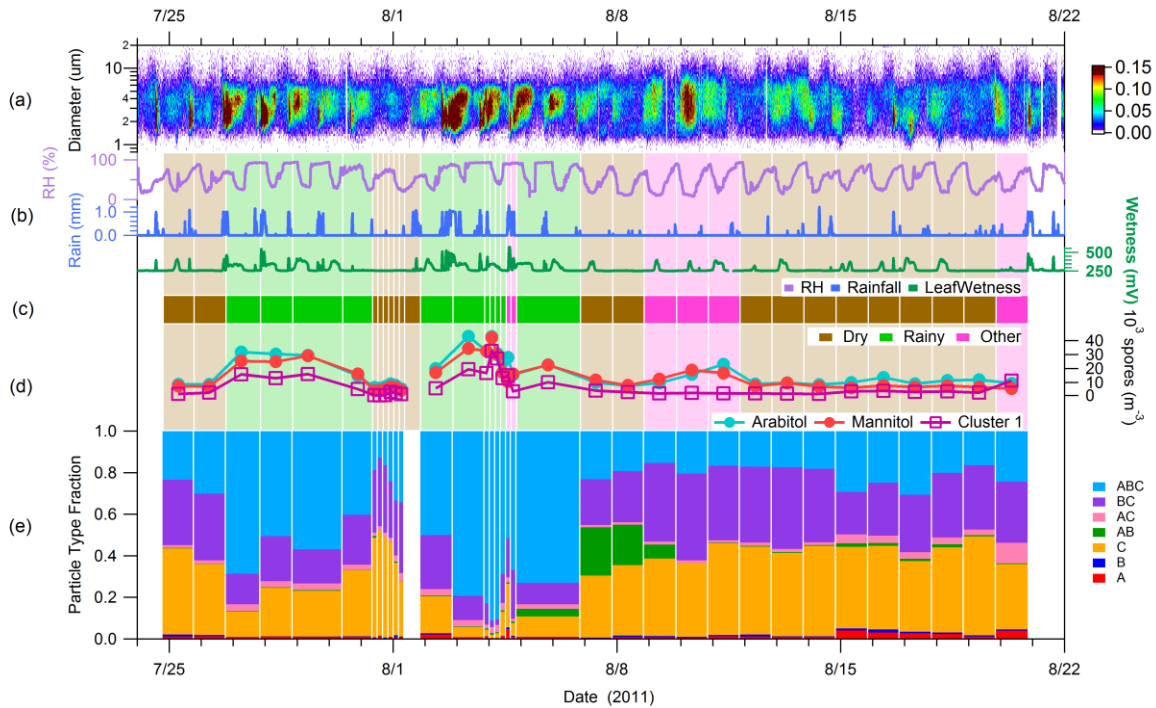
| | | | | | | | |
|------------------------------------|--------------------------|--------------------------|--|--|--|--|--|
| Rainy | 29310 ± 8727 n=11 | 26430 ± 8139 n=11 | | | | | |
| Other | 16850 ± 7415 n=6 | 13350 ± 4863 n=6 | | | | | |
| Fungal Spore Mass Contribution (%) | | | | | | | |
| Dry | 4.81 % ± 1.36 n=18 | 3.72 % ± 1.12 n=18 | | | | | |
| Rainy | 22.88 % ±8.84 n=11 | 20.66 % ±8.49 n=11 | | | | | |
| Other | 9.80 % ± 7.67 n=6 | 7.31 % ± 5.60 n=6 | | | | | |

1009 **Table 3:** Campaign-average concentrations of molecular tracers (measured) and fungal spores (number
1010 concentration estimated from arabitol and mannitol mass). Each set of data broken into wetness
1011 categories. Values are mean ± standard deviation; *n* shows the number of samples used for averaging.
1012 Fungal spore mass contribution was based on the assumption by Bauer et al. (2008b) of 33 pg spore⁻¹.
1013 Total particulate matter mass calculated from UV-APS number concentration (m⁻³) and converted to mass
1014 over aerodynamic particle diameter range 0.5 – 15 µm using density of 1.5 g cm⁻³.

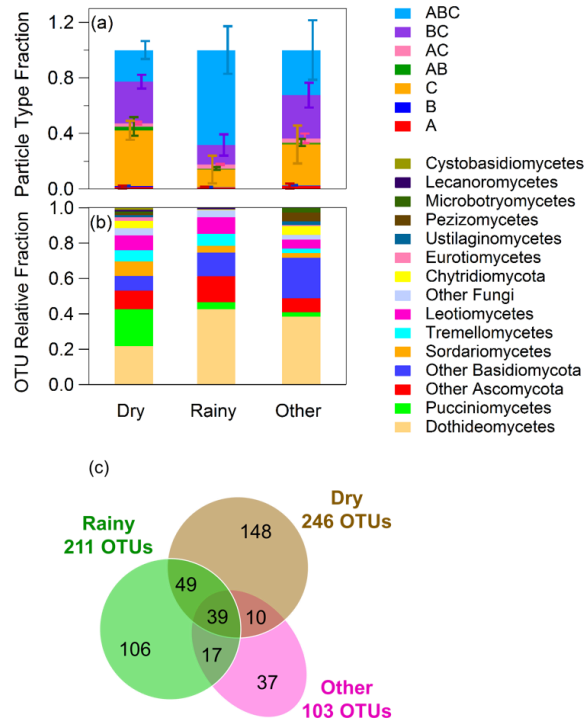


1016
 1017
 1018
 1019
 1020
 1021

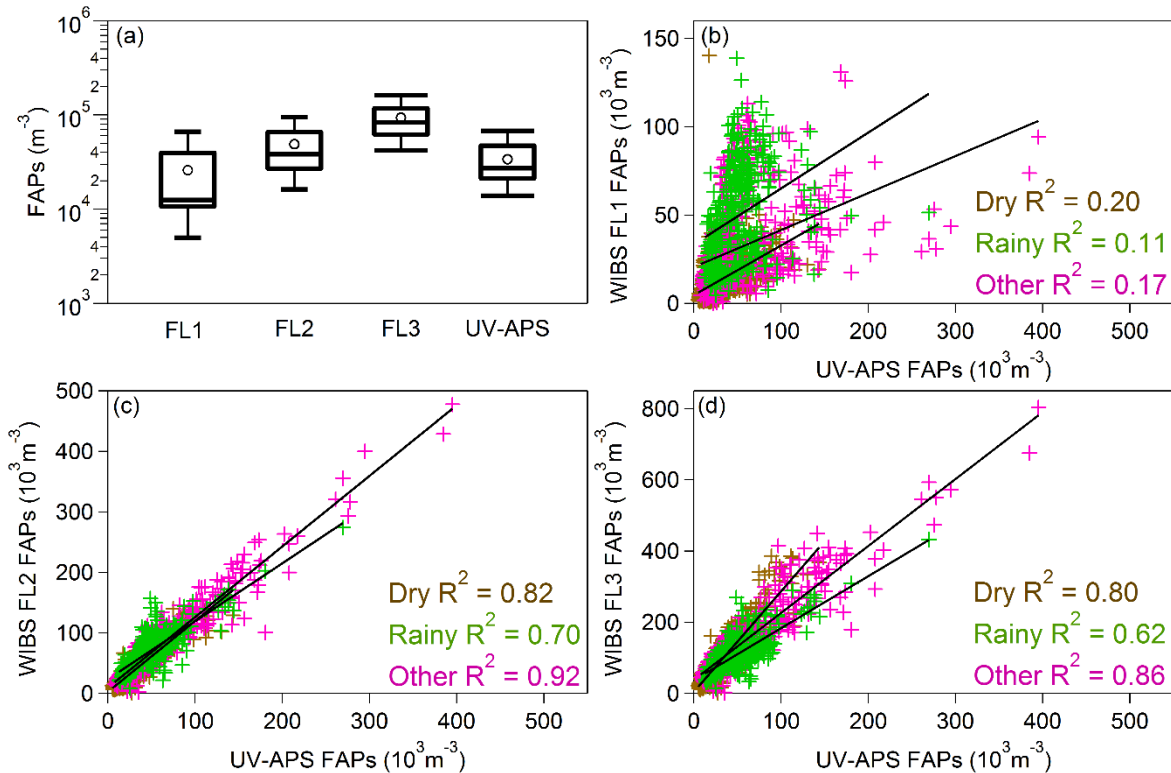
Figure 1: Aerial overview of BEACHON-RoMBAS field site at the Manitou Experimental Forest Observatory located northwest of Colorado Springs, CO. Locations of all instruments and sensors discussed here are marked and were located within a 50 m radius. Figure adapted from Figure 1a of Huffman et al. (2013)



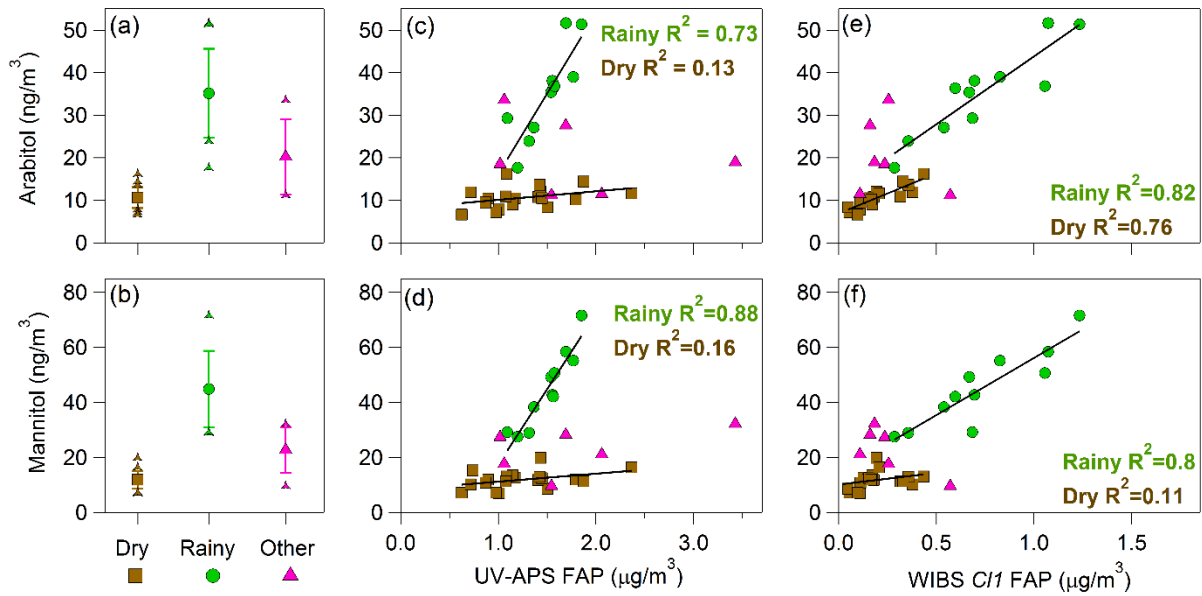
1022
 1023 **Figure 2:** Time series of key species concentrations and meteorological data over entire campaign. (a)
 1024 Fluorescent particle number size distribution measured with UV-APS instrument. Color scale indicates
 1025 fluorescent particle number concentration (L^{-1}). (b) Meteorological data: relative humidity (RH),
 1026 disdrometer rainfall (mm per 15 min), leaf wetness (mV). (c) Wetness category indicated as colored bars;
 1027 green, Rainy; brown, Dry; pink, Other. Bar width corresponds to filter sampling periods. Lightened
 1028 colored bars extend vertically to highlight categorization. (d) Colored traces show fungal spore
 1029 concentrations estimated from molecular tracers (circles) and WIBS C11 data (squares). (e) Stacked bars
 1030 show relative fraction of fluorescent particle type corresponding to each WIBS category.



1031
 1032 **Figure 3:** Characteristic differences between different wetness periods (Dry, Rainy, Other). (a) Relative
 1033 fraction of fluorescent particle number corresponding to each WBS category. Bars show relative standard
 1034 deviation of category fraction in each wetness group (Dry, 19 samples; Rainy, 11 samples; Other, 6
 1035 samples). (b, c) Distribution of fungal OTU (operational taxonomic unit) values. (b) Fungal community
 1036 composition at phylum and class level with Agaricomycetes (dominant class with consistently ~60% of
 1037 diversity) removed. Relative proportion of OTUs assigned to different fungal classes and phyla for each
 1038 sample category shown. (c) Venn diagram showing the number of unique (wetness category specific) and
 1039 shared OTUs (represented by numbers in overlapping areas) among the sample categories (Dry, 11
 1040 samples; Rainy, 7 samples; Other, 3 samples). OTUs classified as cluster of sequences with $\geq 97\%$
 1041 similarity. Taxonomic assignments were performed using BLAST against NCBI database. In total, 3902
 1042 sequences, representing 406 fungal OTUs from 3 phyla and 12 classes were detected. Despite differences
 1043 in community structure across the sample categories, phylogenetic representation appears largely similar.

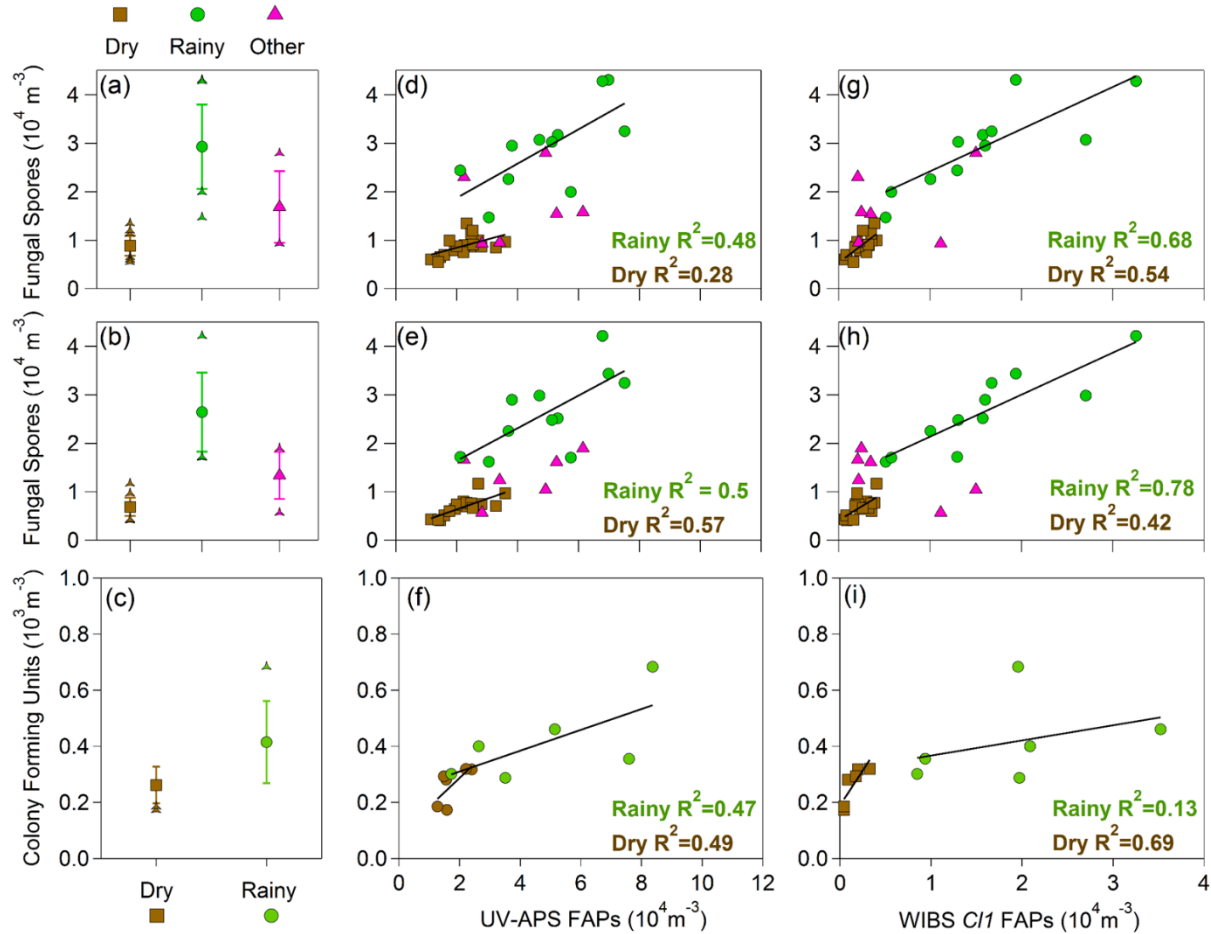


1044
 1045 **Figure 4:** Number concentration of fluorescent particles as a function of instrument channel, averaged
 1046 over entire measurement period. (a) Box-whisker plot of fluorescent particle number concentration for
 1047 WIBS FL1, FL2, FL3, and UVAPS. Circle markers shows mean values, internal horizontal line shows
 1048 median, top and bottom of box show inner quartile, and whiskers show 5th and 95th percentiles. (b) WIBS
 1049 FL1 versus UV-APS (c) WIBS FL2 versus UV-APS (d) WIBS FL3 versus UV-APS. Crosses represent 5-
 1050 minute average points. Linear fits assigned for data in each wetness category.

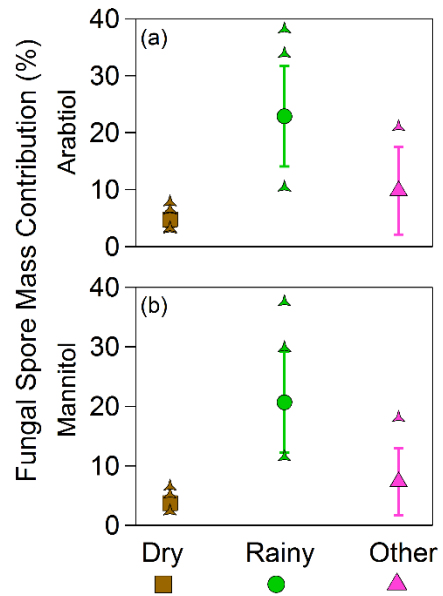


1051
 1052
 1053
 1054
 1055
 1056
 1057
 1058
 1059

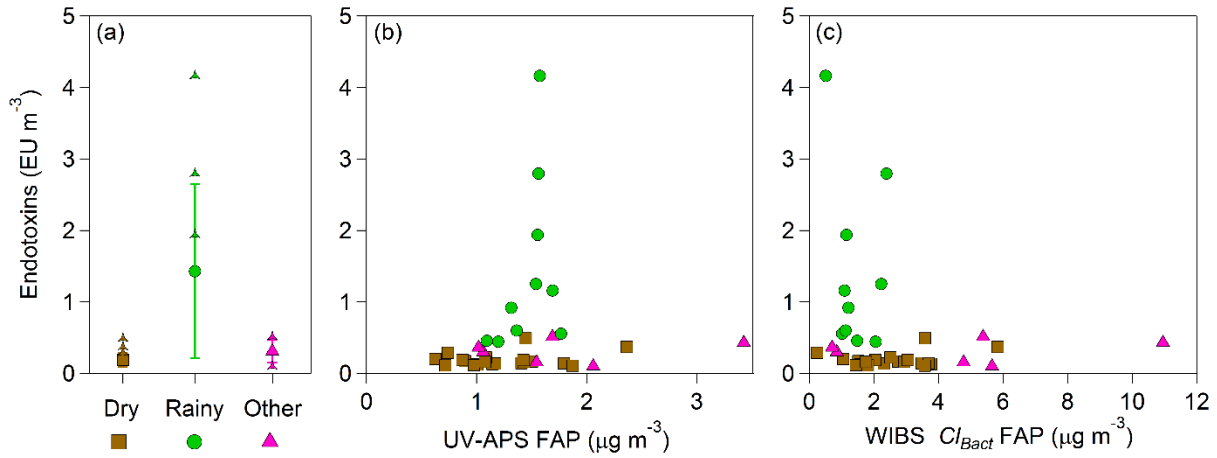
Figure 5: Mass concentrations of molecular tracers and fluorescent particles (assuming unit density particle mass): arabitol – top row, and mannitol – bottom row. Average mass concentration of arabitol (a) and mannitol (b) in each wetness category. Central marker shows mean value of individual filter concentration values, bars represent standard deviation (*s*) range of filter values, and individual points show outliers beyond mean $\pm s$. Correlation of arabitol (c) and mannitol (d) with fluorescent particle mass from UV-APS. Correlation of arabitol I and mannitol (f) with fluorescent particle mass from WIBS Cluster 1. R^2 values shown for each fit in c, d, e, f. Linear fit parameters are shown in Table S2.



1060
 1061 **Figure 6:** Estimated fungal spore number concentration, calculated using mass of arabitol and mannitol
 1062 per spore reported by Bauer et al. (2008a). Estimates from arabitol (top row) and mannitol (middle row).
 1063 Average fungal spore concentration, calculated using arabitol mass (a), mannitol mass (b), and colony
 1064 forming units (c) in each wetness category. Central marker shows mean value of individual filter
 1065 concentration values, bars represent standard deviation (*s*) range of filter values, and individual points
 1066 show outliers beyond mean $\pm s$. Correlation of fungal spore number calculated from arabitol (d) mannitol
 1067 (e), and colony forming units (f) concentration with estimated fluorescent particle mass from UV-APS.
 1068 Correlation of fungal spore number calculated from arabitol (g), mannitol (h), and colony forming unit (i)
 1069 concentration with fluorescent particle concentration from WIBS Cluster 1. R² value shown for each fit
 1070 (right two columns). Linear fit parameters are shown in Table S3.



1071
 1072 **Figure 7:** Estimated fraction of total aerosol mass contributed by fungal spores. Fungal spore mass
 1073 concentration ($\mu\text{g}/\text{m}^3$) calculated separately from mannitol and arabinol concentration and using average
 1074 mass per spore reported by Bauer et al. (2008b). Total particulate matter mass calculated from UV-APS
 1075 number concentration (m^{-3}) and converted to mass over aerodynamic particle diameter range $0.5 - 15 \mu\text{m}$
 1076 using density of 1.5 g cm^{-3} . Central marker shows mean value of individual filter concentration values,
 1077 bars represent standard deviation (s) range of filter values, and individual points show outliers beyond
 1078 $\text{mean} \pm s$.



1080
1081
1082
1083
1084
1085
1086
1087

Figure 8: Endotoxin mass concentration as an approximate indicator of gram-negative bacteria concentration. (a) Averaged concentration in each wetness category. Central marker shows mean value of individual filter concentration values, bars represent standard deviation (*s*) range of filter values, and individual points show outliers beyond mean ± *s*. (b) Correlation of endotoxin mass concentration with estimated fluorescent particle mass from UV-APS. (c) Correlation of endotoxin mass concentration with estimated fluorescent particle mass summed from Clusters 2, 3, and 4 from Crawford et al. (2015).

1088 **Online Supplement for:**

1089

1090 **Title:** Fluorescent Bioaerosol Particle, Molecular Tracer, and Fungal Spore Concentrations during Dry
1091 and Rainy Periods in a Semi-Arid Forest

1092

1093

1094 **Authors:** Marie Ila GOSSELIN^{1,2}, Chathurika M Rathnayake³, Ian Crawford⁴, Christopher Pöhlker²,
1095 Janine Fröhlich-Nowoisky², Beatrice Schmer², Viviane R. Després⁵, Guenter Engling⁶, Martin
1096 Gallagher⁴, Elizabeth Stone³, Ulrich Pöschl², and J. Alex Huffman^{1*}

1097

1098 ¹Department of Chemistry and Biochemistry, University of Denver, Denver, Colorado, USA

1099 ²Max Planck Institute for Chemistry, Multiphase Chemistry and Biogeochemistry Departments, Mainz,
1100 Germany

1101 ³Department of Chemistry, University of Iowa, Iowa City, IA 52246, USA

1102 ⁴Centre for Atmospheric Science, SEAES, University of Manchester, Manchester, UK

1103 ⁵Institute of General Botany, Johannes Gutenberg University, Mainz, Germany

1104 ⁶Division of Atmospheric Sciences, Desert Research Institute, Reno, NV, USA

1105

| Sample Name | Start Time | End Time | Temp (°C) | Relative Humidity (%) | Rain Amount (Normalized) | Leaf Wetness (mV) | FAP Number Ratio (N_f/N_{tot}) | Category |
|-------------|--------------------|--------------------|-----------|-----------------------|--------------------------|-------------------|------------------------------------|----------|
| HiVol 1* | 7/24/2011 18:53 | 7/25/2011 18:00 | 17.833 | 50.185 | 0.002 | 283.040 | 0.058 | Dry |
| HiVol 2 | 7/25/2011 18:07 | 7/26/2011 18:01 | 18.833 | 55.325 | 0.015 | 268.491 | 0.071 | Dry |
| HiVol 3* | 7/26/2011 18:07 | 7/27/2011 18:07 | 15.821 | 62.651 | 0.008 | 308.613 | 0.166 | Rainy |
| HiVol 4 | 7/27/2011 20:00 | 7/28/2011 20:00 | 16.245 | 71.366 | 0.031 | 316.778 | 0.144 | Rainy |
| HiVol 5 | 7/28/2011 20:03 | 7/29/2011 20:03 | 16.143 | 71.328 | 0.000 | 323.439 | 0.102 | Rainy |
| HiVol 6 | 7/30/2011 9:39 | 7/31/2011 7:59 | 18.241 | 64.787 | 0.000 | 265.938 | 0.111 | Rainy |
| HiVol 7* | 7/31/2011 8:02 | 7/31/2011 11:57 | 25.532 | 47.118 | 0.000 | 264.071 | 0.053 | Dry |
| HiVol 8* | 7/31/2011 12:01 | 7/31/2011 16:05 | 28.552 | 60.247 | 0.000 | 261.547 | 0.037 | Dry |
| HiVol 9 | 7/31/2011 16:08 | 7/31/2011 20:04 | 23.847 | 71.358 | 0.000 | 261.640 | 0.045 | Dry |
| HiVol 10* | 7/31/2011 20:06 | 7/31/2011 23:57 | 16.472 | 72.437 | 0.000 | 262.850 | 0.055 | Dry |
| HiVol 11 | 8/1/2011 0:01 | 8/1/2011 4:01 | 14.019 | 47.018 | 0.000 | 264.140 | 0.064 | Dry |
| HiVol 12* | 8/1/2011 4:03 | 8/1/2011 8:03 | 16.829 | 24.150 | 0.000 | 264.600 | 0.061 | Dry |
| HiVol 13 | 8/1/2011 8:06 | 8/1/2011 20:00 | 22.429 | 40.287 | 0.002 | 272.026 | 0.065 | Dry |
| HiVol 14* | 8/1/2011 20:04 | 8/2/2011 20:26 | 14.579 | 59.359 | 0.090 | 323.792 | 0.163 | Rainy |

| | | | | | | | | |
|-----------|--------------------|--------------------|--------|--------|-------|---------|-------|-------------------------------|
| HiVol 15* | 8/2/2011 20:28 | 8/3/2011 20:04 | 15.288 | 83.425 | 0.019 | 319.096 | 0.241 | Rainy |
| HiVol 16 | 8/3/2011 20:06 | 8/4/2011 0:07 | 12.192 | 93.181 | 0.023 | 311.640 | 0.281 | Rainy |
| HiVol 17* | 8/4/2011 0:09 | 8/4/2011 4:10 | 10.120 | 81.078 | 0.000 | 345.847 | 0.348 | Rainy |
| HiVol 18* | 8/4/2011 4:13 | 8/4/2011 8:12 | 12.325 | 45.288 | 0.000 | 316.787 | 0.290 | Rainy |
| HiVol 19* | 8/4/2011 8:15 | 8/4/2011 12:17 | 20.699 | 66.244 | 0.000 | 268.531 | 0.131 | Rainy |
| HiVol 20* | 8/4/2011 12:19 | 8/4/2011 15:57 | 16.594 | 89.947 | 1.088 | 345.723 | 0.114 | Other [†] (Rainy) |
| HiVol 21* | 8/4/2011 16:00 | 8/4/2011 20:12 | 12.355 | 91.505 | 0.021 | 340.625 | 0.189 | Other [†] (Rainy) |
| HiVol 22 | 8/4/2011 20:14 | 8/6/2011 20:03 | 16.309 | 66.855 | 0.001 | 303.368 | 0.170 | Rainy |
| HiVol 23 | 8/6/2011 20:05 | 8/7/2011 20:05 | 19.345 | 46.283 | 0.000 | 280.559 | 0.097 | Dry [†] (Rainy) |
| HiVol 24 | 8/7/2011 20:12 | 8/8/2011 19:48 | 16.486 | 36.066 | 0.000 | 261.572 | 0.072 | Dry |
| HiVol 25 | 8/8/2011 19:49 | 8/9/2011 20:11 | 18.638 | 39.696 | 0.000 | 276.794 | 0.082 | Other |
| HiVol 27 | 8/9/2011 20:13 | 8/10/2011 20:02 | 15.714 | 41.574 | 0.000 | 273.601 | 0.089 | Other |
| HiVol 28 | 8/10/2011 20:05 | 8/11/2011 19:53 | 17.020 | 61.301 | 0.001 | 300.357 | 0.061 | Other [†] (Rainy) |
| HiVol 29 | 8/11/2011 19:54 | 8/12/2011 19:51 | 16.484 | 51.366 | 0.000 | 267.808 | 0.061 | Dry |
| HiVol 30 | 8/12/2011 19:52 | 8/13/2011 19:47 | 17.310 | 52.223 | 0.000 | 291.408 | 0.075 | Dry |

| | | | | | | | | |
|-----------|--------------------|--------------------|--------|--------|-------|---------|-------|-----------------------------|
| HiVol 31 | 8/13/2011 19:48 | 8/14/2011 19:54 | 18.546 | 53.361 | 0.000 | 264.413 | 0.082 | Dry |
| HiVol 32 | 8/14/2011 19:55 | 8/15/2011 20:05 | 17.592 | 57.800 | 0.000 | 281.191 | 0.073 | Dry |
| HiVol 33* | 8/15/2011 20:06 | 8/16/2011 19:47 | 15.037 | 51.222 | 0.003 | 278.961 | 0.080 | Dry |
| HiVol 35* | 8/16/2011 19:48 | 8/17/2011 20:05 | 16.937 | 63.064 | 0.000 | 303.816 | 0.101 | Dry |
| HiVol 36* | 8/17/2011 20:06 | 8/18/2011 19:47 | 18.282 | 55.774 | 0.000 | 295.593 | 0.072 | Dry |
| HiVol 37* | 8/18/2011 19:48 | 8/19/2011 20:07 | 17.883 | 41.821 | 0.000 | 262.093 | 0.074 | Dry |
| HiVol 38* | 8/19/2011 20:08 | 8/20/2011 20:08 | 18.160 | 47.394 | 0.000 | 265.929 | 0.071 | Other [†] (Dry) |

1106

1107 **Table S1:** Summary information for each hi-volume filter sample including: start and stop times (local
1108 time), average air temperature, relative humidity, rain amount (normalized to 2.0) leaf wetness, number
1109 ratio of fluorescent particles from the UV-APS, and wetness category determined as described in Section
1110 3.1. Cross symbol ([†], last column) indicates that category assignment was manually changed from the
1111 algorithm determination (original category in parentheses). Star symbol (*, first column) indicates
1112 samples used in fungal DNA determination. N_f represents the number of fluorescent particles, N_{tot}
1113 represents the number of total particles as measured by the UV-APS.

1114

| Figure | Linear Fit Parameters | |
|--------|-----------------------|---------------|
| | Rainy | Dry |
| 5.c | $y=38.0x-21.8$ | $y=2.0x+8.1$ |
| 5.d | $y=54.9x-37.5$ | $y=2.9x+8.3$ |
| 5.e | $y=32.0x+11.9$ | $y=18.8x+6.9$ |
| 5.f | $y=41.6x+14.6$ | $y=9.9x+9.2$ |

1115

1116 **Table S2:** Linear equation fit parameters for Rainy and Dry conditions for Figure 5c-f. Each equation
1117 represents the linear trend linear for correlations of arabitol (5c,e) or mannitol (5d,f) with UV-APS FAP
1118 mass (5c,d) or WIBS Cl 1 FAP mass (5e,f).

| Figure | Linear Fit Parameters | |
|--------|-----------------------|---------------|
| | Rainy | Dry |
| 6.d | $y=0.4x+11646$ | $y=0.2x+5064$ |
| 6.e | $y=0.3x+9613$ | $y=0.2x+1939$ |
| 6.f | $y=0.004x+236$ | $y=0.01x+83$ |
| 6.g | $y=0.9x+15514$ | $y=1.4x+5389$ |
| 6.h | $y=0.9x+12683$ | $y=1.1x+4094$ |
| 6.i | $y=0.005x+313$ | $y=0.05x+190$ |

1119
1120 **Table S3:** Linear equation fit parameters for Rainy and Dry conditions for Figure 6d-i. Each equation
1121 represents the linear trend linear for correlations of estimated fungal spores ($N\ m^{-3}$) from (6d,g) arabitol,
1122 (6e,h) mannitol or (6f,i) colony forming units (CFU) with (6d,e,f) UV-APS FAPs or (6g,h,i) WIBS Cl 1
1123 FAPs.

| Particle Mass Percentage (%) | | | |
|--|--------------------|--------------------|--------------------|
| | Dry | Rainy | Other |
| CI1 | 2.15 ± 1.38 | 16.98 ± 10.14 | 4.03 ± 3.42 |
| CI2 | 4.72 ± 1.43 | 6.01 ± 1.57 | 6.68 ± 2.38 |
| CI3 | 19.92 ± 5.81 | 13.22 ± 5.78 | 23.79 ± 10.60 |
| CI4 | 4.44 ± 1.64 | 8.83 ± 3.73 | 6.53 ± 3.45 |
| FL 1 | 8.42 ± 3.37 | 62.05 ± 35.10 | 24.70 ± 23.61 |
| FL 2 | 18.51 ± 4.02 | 71.55 ± 31.34 | 38.26 ± 24.77 |
| FL 3 | 36.79 ± 6.26 | 85.95 ± 28.23 | 61.77 ± 28.29 |
| FL | 38.01 ± 6.34 | 87.99 ± 28.53 | 64.92 ± 30.66 |
| UVAPS FAP | 25.53 ± 2.99 | 51.50 ± 14.83 | 32.87 ± 9.45 |
| Total Particle Mass ($\mu\text{g m}^{-3}$) | | | |
| UVAPS Total | 3.70 ± 1.11 | 2.70 ± 0.58 | 4.85 ± 2.56 |

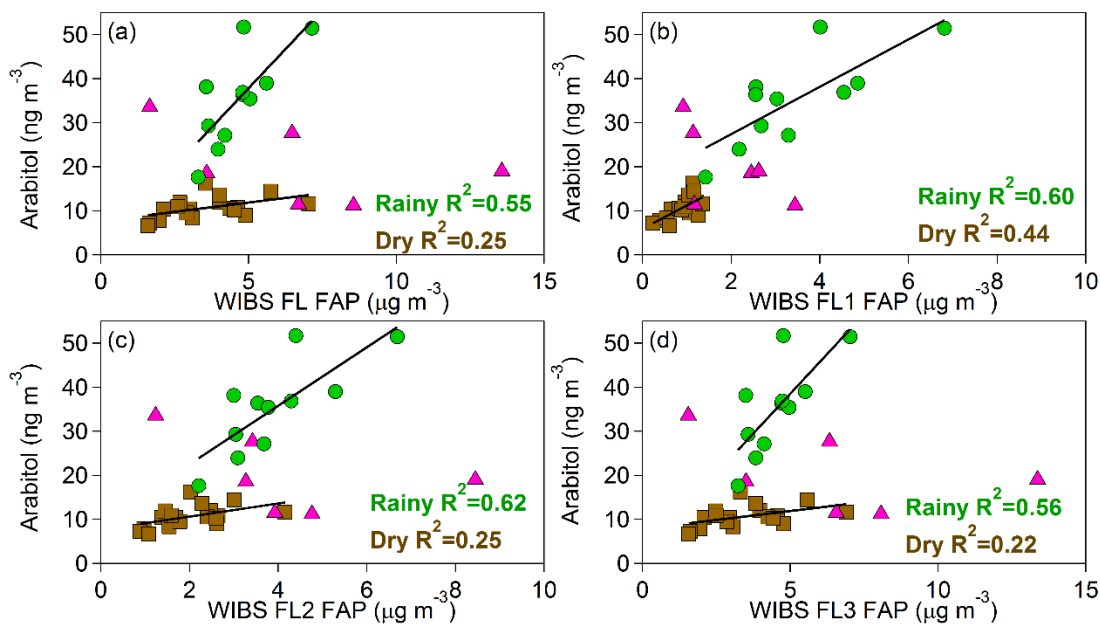
1124

1125 **Table S4:** Percentage of particle mass in various UV-LIF instrument categories **and total particle mass.**
1126 Each mass value compared to total particle mass, determined using UV-APS number size distributions,
1127 converted to a mass for particles of aerodynamic diameter 0.5 – 10 μm and using particle mass density of
1128 unity. WIBS particles were integrated into total number over the same size range in optical diameter and
1129 using unity density. Range shown are standard deviation of 5-minute time averages.

| Particle Type | FL1 Fluorescence Intensity | FL2 Fluorescence Intensity | FL3 Fluorescence Intensity |
|---------------|----------------------------|----------------------------|----------------------------|
| A | I>Threshold | | |
| B | | I>Threshold | |
| C | | | I>Threshold |
| AB | I>Threshold | I>Threshold | |
| AC | I>Threshold | | I>Threshold |
| BC | | I>Threshold | I>Threshold |
| ABC | I>Threshold | I>Threshold | I>Threshold |

1130
1131
1132
1133
1134
1135

Figure S1: Particle type assignment for WIBS data. Particle category type defined as fluorescent in a given channel when the fluorescence intensity (I) in channel FL1, FL2, or FL3 is greater than the threshold value, defined as blank + 3 σ . Colors correspond to particle type used also in Figures 2-3.



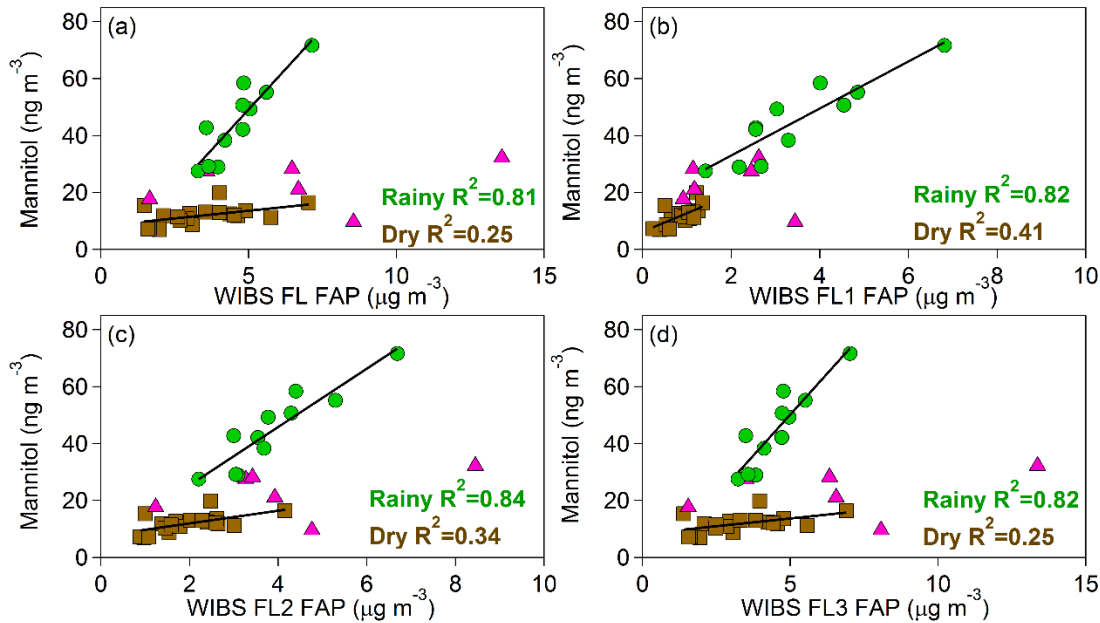
1136
1137
1138
1139
1140
1141

Figure S2: Atmospheric arabinol concentration (ng m^{-3}) correlated with WIBS fluorescent particle mass ($\mu\text{g m}^{-3}$) (a) any fluorescent particle, FL; (b) particles fluorescent in channel 1, FL1; (c) particles fluorescent in channel 2, FL2; (d) particles fluorescent in channel 3, FL3. R^2 value shown for each fit in a,b,c,d. Linear fit parameter are shown in the table below.

| Figure | Linear Fit Parameters | |
|--------|-----------------------|---------------|
| | Rainy | Dry |
| S2.a | $y=7.1x+2.4$ | $y=0.8x+7.6$ |
| S2.b | $y=5.4x+16.7$ | $y=5.3x+5.9$ |
| S2.c | $y=6.6x+9.2$ | $y=1.5x+7.6$ |
| S2.d | $y=7.2x+2.4$ | $y=0.81x+7.8$ |

1142

1143 Linear equation fit parameters for Rainy and Dry conditions for Figure S2a-d. Each equation represents
1144 the linear trend linear for correlations of arabinol (ng m^{-3}) with WIBS fluorescent channel particle mass
1145 ($\mu\text{g m}^{-3}$). (a) any fluorescent particle, FL; (b) particles fluorescent in channel 1, FL1; (c) particles
1146 fluorescent in channel 2, FL2; (d) particles fluorescent in channel 3, FL3.



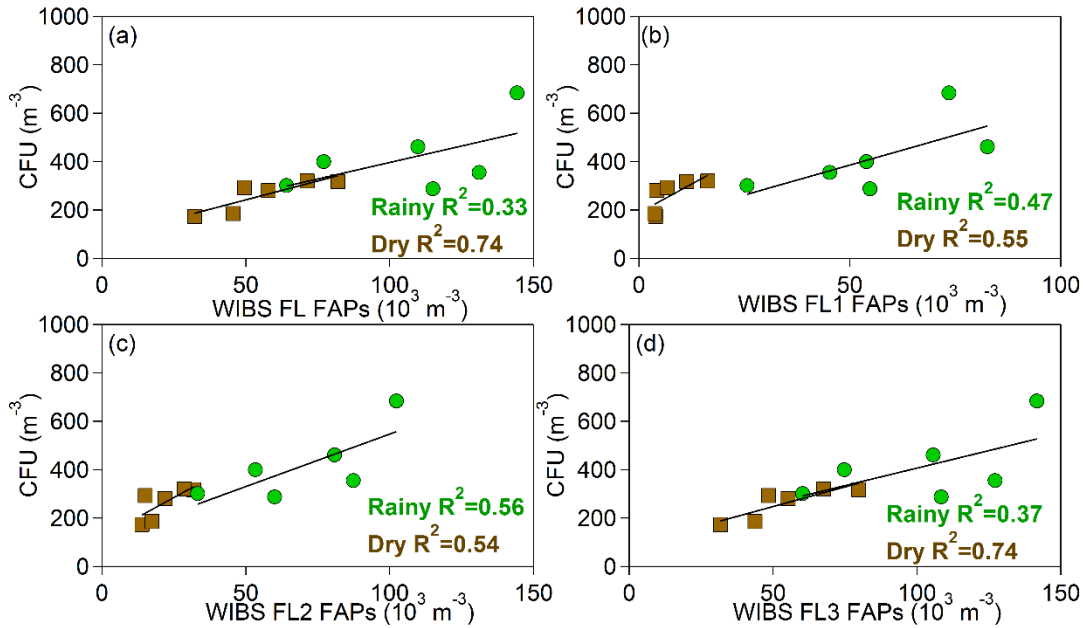
1147

1148 **Figure S3:** Atmospheric mannitol concentration (ng m^{-3}) correlated with WBS fluorescent particle
 1149 mass ($\mu\text{g m}^{-3}$) (a) any fluorescent particle, FL; (b) particles fluorescent in channel 1, FL1; (c) particles
 1150 fluorescent in channel 2, FL2; (d) particles fluorescent in channel 3, FL3. R^2 value shown for each fit in
 1151 a,b,c,d. Linear fit parameter are shown in the table below.
 1152

| Figure | Linear Fit Parameters | |
|--------|-----------------------|--------------|
| | Rainy | Dry |
| S3.a | $y=11.3x-7.5$ | $y=1.1x+8.2$ |
| S3.b | $y=8.3x+16.4$ | $y=6.5x+6.2$ |
| S3.c | $y=10.3x+4.9$ | $y=2.2x+7.5$ |
| S3.d | $y=11.5x-7.4$ | $y=1.1x+8.2$ |

1153

1154 Linear equation fit parameters for Rainy and Dry conditions for Figure S3a-d. Each equation represents
 1155 the linear trend linear for correlations of mannitol (ng m^{-3}) with WBS fluorescent channel particle mass
 1156 ($\mu\text{g m}^{-3}$). (a) any fluorescent particle, FL; (b) particles fluorescent in channel 1, FL1; (c) particles
 1157 fluorescent in channel 2, FL2; (d) particles fluorescent in channel 3, FL3.



1158

1159 **Figure S4:** Atmospheric colony forming unit (CFU) concentration (CFU m⁻³) correlated with WBS
 1160 fluorescent particle (m⁻³) (a) any fluorescent particle, FL; (b) particles fluorescent in channel 1, FL1; (c)
 1161 particles fluorescent in channel 2, FL2; (d) particles fluorescent in channel 3, FL3. R² value shown for
 1162 each fit in a,b,c,d. Linear fit parameter are shown in the table below.
 1163

| Figure | Rainy Linear Parameters | Dry Linear Parameters |
|--------|-------------------------|-----------------------|
| S4.a | $y=0.003x+124$ | $y=0.003x+86$ |
| S4.b | $y=0.005x+138$ | $y=0.009x+189$ |
| S4.c | $y=0.004x+113$ | $y=0.006x+122$ |
| S4.d | $y=0.003x+118$ | $y=0.003x+84$ |

1164

1165 Linear equation parameters for Rainy and Dry conditions for Figure S3a-d. Each equation represents the
 1166 linear trend linear for correlations of colony forming units (CFU m⁻³) with WBS fluorescent channel
 1167 particles (N m⁻³). (a) any fluorescent particle, FL; (b) particles fluorescent in channel 1, FL1; (c) particles
 1168 fluorescent in channel 2, FL2; (d) particles fluorescent in channel 3, FL3.

1169